



# Anthropogenic and biogenic influence on VOC fluxes at an urban background site in Helsinki, Finland

Pekka Rantala<sup>1</sup>, Leena Järvi<sup>1</sup>, Risto Taipale<sup>1</sup>, Terhi K. Laurila<sup>1</sup>, Johanna Patokoski<sup>1</sup>, Maija K. Kajos<sup>1</sup>, Mona Kurppa<sup>1</sup>, Sami Haapanala<sup>1</sup>, Erkki Siivola<sup>1</sup>, Taina M. Ruuskanen<sup>1</sup>, and Janne Rinne<sup>1,2,3</sup>

<sup>1</sup>Department of Physics, University of Helsinki, Helsinki, Finland

<sup>2</sup>Department of Geoscience and Geography, University of Helsinki, Helsinki, Finland

<sup>3</sup>Finnish Meteorological Institute, Helsinki, Finland

*Correspondence to:* Pekka Rantala (pekka.a.rantala@helsinki.fi)

**Abstract.** We measured volatile organic compounds (VOC), carbon dioxide (CO<sub>2</sub>) and carbon monoxide (CO) at an urban background site near the city centre of Helsinki, Finland, Northern Europe. The VOC and CO<sub>2</sub> measurements were obtained between January 2013 and September 2014 whereas for CO a shorter measurement campaign in April–May 2014 was conducted. Both anthropogenic and biogenic sources were identified for VOCs in the study. Strong correlations between VOC fluxes and CO fluxes and traffic rates indicated anthropogenic source of many VOCs. The VOC with highest emission to the atmosphere was methanol which originated mostly from traffic and other anthropogenic sources. Traffic was also a major source for aromatic compounds in all seasons whereas isoprene was mostly emitted from biogenic sources during summer. Small traffic related isoprene emissions were detected during other seasons. Generally, the VOC fluxes were found to be small compared with previous urban VOC flux studies. However, the differences were probably caused by lower anthropogenic activities as the CO<sub>2</sub> fluxes were also relatively small at the site.

## 1 Introduction

Micrometeorological flux measurements of volatile organic compounds (VOC) in urban and semi-urban areas are limited, although local emissions have major effect on the local and regional atmospheric chemistry and furthermore on air quality (e.g. Reimann and Lewis, 2007 and references therein). Biogenic VOCs, mainly isoprene and monoterpenes, affect hydroxyl radical (OH) concentration, particle growth, and formation of photochemical oxidants (Atkinson, 2000; Atkinson and Arey, 2003; Kulmala et al., 2004; Spracklen et al., 2008; Kazil et al., 2010; Paasonen et al., 2013). Long-lived compounds, such as anthropogenically emitted benzene, contribute also to VOC concentrations in rural areas (e.g. Patokoski et al., 2014, 2015).

VOCs may have both anthropogenic and biogenic sources in urban areas which complicates the analysis of VOC flux measurements made in these areas. Globally, most important anthropogenic sources are traffic, industry, gasoline evaporation and solvent use (Watson et al., 2001; Reimann and Lewis, 2007; Kansal, 2009; Langford et al., 2009; Borbon et al., 2013 and references therein) whereas biogenic VOC sources within cities include mostly urban vegetation, such as trees and shrubs in public parks and at street canyons. Based on previous micrometeorological flux studies, urban areas are observed to be a source for methanol, acetonitrile, acetaldehyde, acetone, isoprene, benzene, toluene and C<sub>2</sub>-benzenes (Velasco et al., 2005;



Filella and Peñuelas, 2006; Langford et al., 2009; Velasco et al., 2009; Langford et al., 2010; Park et al., 2013; Valach et al., 2015). In addition, concentration measurements connected to source models have shown emissions of various other VOCs, such as light hydrocarbons, from urban sources (e.g. Watson et al., 2001; Hellén et al., 2003, 2006, 2012). Monoterpene emissions have surprisingly remained mainly unstudied, although monoterpenes have generally major effect on the atmospheric chemistry. For example, Hellén et al. (2012) found that monoterpenes and isoprene together have a considerable role in OH-reactivity in Helsinki, Southern Finland. Biogenic emissions might have also a considerable role in ozone ( $O_3$ ) chemistry in urban areas (e.g. Calfapietra et al., 2013).

The VOC flux measurements reported in literature have been conducted in the latitudes ranging from  $19^\circ N$  to  $53^\circ N$ , but most of the measurement in the north have been conducted in British Isles with their relatively mild winters. Thus no measurements have been reported from northern continental urban areas. VOC emissions from traffic are typically due to incomplete combustion. This also results in emissions of carbon monoxide (CO), and thus the emissions of certain VOCs are potentially linked with CO fluxes. However, only one of the publications on urban VOC fluxes mentioned above combine the VOC fluxes with CO fluxes in their analysis. Thus our aim is to i) characterize the VOC fluxes in a northern urban city over an annual cycle, ii) to identify the main sources, such as traffic and vegetation, of aromatics, oxygenated VOCs and terpenoids using traffic counts, measured CO and carbon dioxide ( $CO_2$ ) fluxes and the ambient temperature ( $T$ ), and iii) compare the VOC fluxes with previous urban VOC flux studies to assess the relation of VOC fluxes to CO and  $CO_2$  fluxes in different cities.

## 2 Materials and methods

### 2.1 Measurement site and instrumentation

Measurements were carried out at urban background station SMEAR III in Helsinki ( $60^\circ 12' N$ ,  $24^\circ 58' E$ ). The population of Helsinki is around 630 000 (<http://vrk.fi/default.aspx?docid=8882&site=3&id=0>, cited in 12 Dec 2015). The site is classified as local climate zone 6 (Stewart and Oke, 2012) and it belongs to the humid continental climate zone with clear annual variations between four seasons: the monthly mean temperature varies from  $-4.9^\circ C$  in February to  $17.6^\circ C$  in July (1971–2000, Drebs et al., 2002; see also Fig. 1), and daylight hours range from 6 to 19 h per day. SMEAR III consists of a 31-m-tall lattice tower located on a hill, 26 m above the sea level and 19–21 m above the surrounding terrain. The site is roughly five kilometres North-East from the Helsinki City Centre. According to the wind direction, the measurement surroundings around the tower can be divided into three areas: built, road and vegetation (Vesala et al., 2008, Table 1, Fig. 2).

The built sector in the northern direction ( $320^\circ$ – $40^\circ$ ) is dominated by university campus buildings and the Finnish Meteorological Institute (mean height 20 m) close to the tower. In the road sector ( $40^\circ$ – $180^\circ$ ), one of the main roads leading to Helsinki city centre passes through with the closest distance between the road and the tower being 150 m. The area in-between is covered by deciduous forest with mainly birch (*Betula sp.*), Norway maple (*Acer platanoides*), aspen (*Populus tremula*), goat willow (*Salix caprea*) and bird cherry (*Prunus padus*) (Vesala et al., 2008, Fig. 2). On the road, a typical workday traffic rate is around 44 000 vehicles per day (Lilleberg and Hellman, 2011), and the vehicles have been found to be the main source of  $CO_2$  and aerosol particle emissions in the area (Järvi et al., 2012; Ripamonti et al., 2013). In the vegetation sector ( $180^\circ$ – $320^\circ$ ), most of



the surface is covered by green areas of the Kumpula Botanic Garden and the City Allotment Garden. During this study, the wind blew most often from the vegetation sector and least from the built sector.

The site infrastructure, flux measurement conditions and surrounding areas are described in detail by Vesala et al. (2008) and Järvi et al. (2009a).

### 5 2.1.1 VOC measurements with PTR-MS and volume mixing ratio calculations

A proton-transfer-reaction quadrupole mass spectrometer (PTR-MS, Ionicon Analytik GmbH, Innsbruck, Austria; Lindinger et al., 1998) was measuring 12 different mass-to-charge ratios ( $m/z$ , see Table 2) every second hour using a 0.5 s sampling time between 1 January 2013 and 27 June 2014 (Fig. 1). Rest of the time the PTR-MS sampled a wider range of mass-to-charge ratios from one level but those measurements are not considered in this study. In addition, we had a short campaign between 27 June and 30 September 2014 when 14 mass-to-charge ratios were measured using the same 0.5 s sampling time. During the campaign, those two additional mass-to-charge ratios were  $m/z$  89 and  $m/z$  103. In that period, the measurement cycle took always two hours so that  $m/z$  31–69 were measured during the first and  $m/z$  79–137 during the second hour. In summer 2014, there were some gaps due to software problems (Table 2).

The PTR-MS was located inside a measurement cabin and sample air was drawn to the instrument using a PTFE tubing with 8 mm inner diameter (i.d.). The sample line was 40-m-long and it was heated ( $10 \text{ W m}^{-1}$ ) to avoid condensation of water vapour. A continuous air-flow was maintained in the tube with some variations in the flow rate: first  $20 \text{ l min}^{-1}$  (whole year 2013), then  $40 \text{ l min}^{-1}$  (until 30 May 2014) and then  $20 \text{ l min}^{-1}$  (until the end of the measurements) again. From the main inlet, a side flow of  $50\text{--}100 \text{ ml min}^{-1}$  was drawn to PTR-MS via a 0.5-m-long PTFE tube with 1.6 mm i.d.

The PTR-MS was maintained at a drift tube pressure of 2.0–2.2 mbar and primary ion ( $\text{H}_3\text{O}^+$ ) count rate of about  $10\text{--}30 \cdot 10^6$  cps (measured at  $m/z$  21).  $E/N$ -ratio where  $E$  is the electric field and  $N$  the number density of the gas in the drift tube, was typically around 135 Td ( $\text{Td} = 10^{-21} \text{ V m}^2$ ). The oxygen level  $\text{O}_2^+$  was mostly below 2% of the  $\text{H}_3\text{O}^+$  signal.

The instrument was calibrated every second or third week using a diluted VOC standard (Apel-Riemer, Table 2). The volume mixing ratios were calculated using the procedure described in detail by Taipale et al. (2008). Before a calibration, the SEM voltage (MasCom MC-217) of the PTR-MS was always optimized to get a correct primary ion signal level (e.g. Kajos et al., 2015). The instrumental background was determined every second hour by measuring VOC free air, produced with a zero air generator (Parker Balzon HPZA-3500-220). The intake for the zero air generator was outside of the measurement cabin close to the ground. During the measurement period, the zero air generator was working sometimes improperly leading to contaminated  $m/z$  93 signal. These periods were removed from the zero air measurements and replaced by nearest reliable values. In addition, due to software problems, the zero air measurements were not recorded between 7 July and 30 September 2014. These gaps were replaced by a median diurnal cycle values of the zero air measured during 27 June – 7 July 2014. One should note that the mentioned problems with the zero air measurements had no effect on flux calculations. However, they did, of course, cause some uncertainties for the measured concentration levels.



## 2.1.2 Ancillary measurements and data processing

An ultrasonic anemometer (Metek USA-1, Metek GmbH, Germany) was installed at 31 m, 0.13 m above the VOC sampling inlet. The ambient temperature was also measured at the VOC sampling level with a Pt-100 sensor. The photosynthetic photon flux density was measured at 31 m in the measurement tower using a photodiode sensor (Kipp&Zonen, Delft, Netherlands).

5 Pressure was measured with Vaisala HMP243 barometer on the roof of the University building near the site.

Hourly traffic rates were measured online 4 km from the measurement site by the City of Helsinki Planning Department. These rates were converted to correspond to traffic rates on the road next to the measurement site following the procedure by Järvi et al. (2012).

CO<sub>2</sub> and CO concentrations (10 Hz) were measured with a Li-Cor 7000 (LI-COR, Lincoln, Nebraska, USA) and the  
10 CO/N<sub>2</sub>O analyser (Los Gatos Research, model N2O/CO-23d, Mountain View, CA, USA; later referred as LGR), respectively. CO<sub>2</sub> concentration was measured continuously between January 2013 and September 2014. The CO concentration was measured between 3 April and 27 May 2014 (Fig. 1) and the LGR was connected to the same main inlet line with the PTR-MS. During the CO measurements, the main inlet flow was 40 l min<sup>-1</sup>. After the LGR was removed from the setup, the main inlet flow was decreased to 20 l min<sup>-1</sup> to increase the pressure in the sampling tube and to get a higher side flow to the PTR-MS  
15 (from 50 to 100 ml min<sup>-1</sup>).

Thirty minute average CO and CO<sub>2</sub> fluxes were calculated using the eddy covariance technique from the raw data according to commonly accepted procedures (Aubinet et al., 2012). A two-dimensional (2D) coordinate rotation was applied to the wind data and all data were linearly de-trended. 2D rotation was used instead of the planar fitting as the 2D rotation is likely to be less prone to systematic errors above a complex urban terrain (Nordbo et al., 2012b). Spike removal was made based  
20 on the difference limit (Mammarella et al., 2015). Time lags between wind and scalar data were obtained by maximizing the cross-covariance function. For CO and CO<sub>2</sub>, mean time lags of 5.8 s and 7.0 s, respectively, were obtained. Finally, spectral corrections were applied. The low frequency losses for both fluxes were corrected based on theoretical corrections (Rannik and Vesala, 1999), whereas the high-frequency losses were experimentally determined. Finally, the 30-min fluxes were quality checked for stationarity with a limit of 0.3 (Foken and Wichura, 1996), and periods with  $u_* < 0.2 \text{ m s}^{-1}$  were  
25 removed from further analysis. More details of the data post-processing can be found in Nordbo et al. (2012b). Data coverages for CO and CO<sub>2</sub> fluxes were 54.0% and 61.9%, respectively.

## 2.2 VOC flux calculations

### 2.2.1 Disjunct eddy covariance method

In the disjunct eddy covariance method (hereafter DEC), the flux is calculated using a discretized covariance:

$$30 \quad \overline{w'c'} \approx \frac{1}{n} \sum_{i=1}^n w'(i - \lambda/\Delta t)c'(i), \quad (1)$$

where  $n$  is the number of measurements during the flux averaging time,  $\Delta t$  is the sampling interval and  $\lambda$  is a lag time caused by sampling tubes (e.g. Rinne et al., 2001; Karl et al., 2002; Rinne and Amman, 2012). The fluxes measured by the DEC



method suffer from same sources of systematic underestimation as the fluxes measured by the EC method, including high and low frequency losses (e.g. Moore, 1986; Horst, 1997). According to Horst (1997), the high frequency losses,  $\alpha_{\text{horst}}$ , can be estimated using an equation

$$(\alpha_{\text{horst}})^{-1} = \frac{1}{1 + (2\pi f_m \tau)^\beta}, \quad (2)$$

- 5 where  $\tau$  is the response time of the system,  $f_m = n_m \bar{u} / (z_m - d)$  and  $\beta = 7/8$  and  $\beta = 1$  in unstable and stable stratification, respectively. In here,  $\bar{u}$  is the mean horizontal wind,  $z_m$  the measurement height and  $d$  a zero displacement height. The parameter  $n_m$  has been observed to be constant in unstable stratification at the site ( $n_m = 0.1$ ), and in stable stratification ( $\zeta > 0$ ) having the following experimental, stability and wind direction dependent values (Järvi et al., 2009b):

$$n_m = \begin{cases} 0.1(1 + 2.54\zeta^{0.28}), & d = 13 \text{ m, (built)} \\ 0.1(1 + 0.96\zeta^{0.02}), & d = 8 \text{ m, (road)} \\ 0.1(1 + 2.00\zeta^{0.27}), & d = 6 \text{ m, (vegetation)} \end{cases} \quad (3)$$

- 10 where  $\zeta$  is the stability parameter.

VOC fluxes were calculated for each 45-min-period according to Eq. (1). Before the calculations, a linear trend was removed from the concentration and wind measurements. In addition, 2D rotation was applied to the wind vectors.

- The PTR-MS and the wind data were recorded to separate computers, thus, lag times were shifting artificially as the computer clocks performed unequally. Therefore, we first determined lag times of  $m/z$  37 (first water cluster,  $\text{H}_3\text{O}^+\text{H}_2\text{O}$ ) for each data  
15 set between two calibrations. Then, a linear trend was removed from the lag times to cancel the artificial shift. After that, the shifted cross covariance functions were summed (as in Park et al., 2013), and an average lag-time was determined for each mass-to-charge ratio from the summed cross covariance functions. Finally, a lag-time for each 45-min-period was determined by using a  $\pm 2.5$  s lag time window around the previously determined mean lag-time, and a smoothed maximum covariance method described by Taipale et al. (2010). However, if the mean lag-time value was not found, the previous reliable mean lag-  
20 time value was used instead. We defined that a mean lag-time was representative if a peak value of a summed cross covariance function was higher than  $3\sigma_{\text{tail}}$  where  $\sigma_{\text{tail}}$  is the mean standard deviation of the summed cross covariance function tails. The standard deviations were calculated using lag-time windows  $\pm(180 - 200)$  s. If a mass-to-charge ratio showed no representative peak values at all, its flux values were defined to be insignificant.

- The lag times were allowed to vary slightly ( $\pm 2.5$  s) around the mean lag-times because removing the linear trend potentially  
25 caused uncertainties. Moreover, changes in relative humidity might have led to changes in the lag times at least in the case of methanol which is a water-soluble compound, even with heated inlet line. However, the lag time window we used was quite narrow,  $\pm 2.5$  s, to limit uncertainties ("mirroring effect") caused by the maximum covariance method connected to the fluxes near the detection limit (Langford et al., 2015). Also, one should note that in our case the maximum was determined from the smoothed cross covariance function which already limits the possible overestimation of the measured DEC fluxes, and thus the  
30 mirroring effect (Taipale et al., 2010).



Constant response time of 1.0 s and Eq. (2) were used for the high-frequency flux corrections. The constant value was estimated based on previous studies with PTR-MS (Ammann et al., 2006; Rantala et al., 2014; Schallhart et al., 2015) where the response time of the measurement setup was estimated of being around 1 s. However, the response time is probably compound dependent as e.g. methanol might have a dependence on the relative humidity (RH) because it is a polar molecule. The response time of water vapour has been observed to increase as a function of RH (e.g. Ibrom et al., 2007; Mammarella et al., 2009; Nordbo et al., 2012b) and this is likely for methanol as well. In addition, the length of the sampling tube affects the response time as well but the effect is difficult to quantify without experimental data (Nordbo et al., 2013).

The correction factor  $\alpha_{\text{horst}}$  was on average 1.16. Even though the use of constant value of  $\tau = 1.0$  s may lead to random uncertainties if the true response time varies temporally, this is likely to have only a small effect on the calculated fluxes. Also a systematic error of a few percentages is possible if the actual average response time was smaller or higher. We can also note that the change of the flow rate from 20 to 40 l min<sup>-1</sup> had only a negligible effect on the attenuation as long as the flow is turbulent (see Nordbo et al., 2014).

In addition to the high frequency losses, the calculated flux values may also be biased by some other factors. For short-lived isoprene and monoterpenes (minimum lifetimes ca. 2 hours, see Hellén et al., 2012), the flux losses due to chemical degradation were estimated to be few percentages (see Rinne et al., 2012). However, these losses are difficult to compensate as they do depend on oxidant concentrations (mainly OH and O<sub>3</sub>) and the surface layer mixing. Thus, no corrections due to the chemical degradation were applied. All flux values are also slightly underestimated as low frequency corrections were left out due to noisy VOC spectra. Larger errors might be produced by calibration uncertainties that affect directly on the measured fluxes. All mass-to-charge ratios excluding  $m/z$  47 (ethanol+formic acid) were directly calibrated in this study, but according to Kajos et al. (2015), concentrations of calibrated compounds may also be biased due to unknown reasons. Flux values of ethanol+formic acid should especially be considered with caution as the concentrations of  $m/z$  47 signal were determined from transmission curves (see Taipale et al., 2008).

Periods when the anemometer or the PTR-MS were working improperly, were removed from the time series (Fig. 1). For example, fluxes were not measured during summer 2013 due to a thunderstorm that broke the anemometer, and in the beginning of 2014, the PTR-MS was serviced in a laboratory. During some periods, signal levels did not behave normally but had for example a lot of spikes. Thus those periods were disregarded as well. To limit the underestimation of absolute flux values caused by a weak mixing, the fluxes during which  $u_* < 0.2$  m s<sup>-1</sup> were also rejected from further analysis. Other quality controlling, such as filtering flux data with flux detection limits or with the stationarity criteria (Foken and Wichura, 1996), was not performed because applying these methods for the noisy DEC data would potentially bring other uncertainty sources. However, before calculating correlation coefficients between a VOC and another compound (CO, CO<sub>2</sub> or a VOC), a percentage (1%) of the lowest and highest values were removed to avoid effect of possible outliers. Data coverages for VOCs are listed in Table 2.



### 2.2.2 Identification of measured mass-to-charge ratios

Identifications of the measured mass-to-charge ratios are listed in Table 2. Most of the identifications are clear but there are some exceptions. First of all, p-cymene fragments to the same  $m/z$  93 with toluene (Tani et al., 2003). Therefore, p-cymene may potentially have had an influence on the observed concentrations at  $m/z$  93 as the used  $E/N$ -ratio, 135 Td, caused probably fragmentation of p-cymene (Tani et al., 2003). However, Hellén et al. (2012) observed that p-cymene concentrations at the SMEAR III site are low compared with the toluene concentrations, around 9% during July. Therefore, the major compound at  $m/z$  93 was likely toluene, although p-cymene might have increased flux at  $m/z$  93 during warm days.

Anthropogenic furan (de Gouw and Warneke, 2007) had probably a major contribution on the measured  $m/z$  69 concentrations between October and May when isoprene concentrations at the site have been reported to be small (around 5 – 30 ppt; Hellén et al., 2006, 2012). In our study, mean  $m/z$  69 concentrations between June and August were only ca. 60% larger than during other seasons (Table 3), indicating considerable influence of furan. Another important compound influencing measurements at  $m/z$  69 is methylbutenol (MBO) fragment (e.g. Karl et al., 2012). However, MBO is mostly emitted from conifers (e.g. Guenther et al., 2012) that are rare near the SMEAR III station. Therefore, MBO should have had only a negligible effect on the concentration and fluxes measured at  $m/z$  69.

Monoterpenes fragment to the  $m/z$  81. The parental mass-to-charge ratio of monoterpenes,  $m/z$  137, had low sensitivity during the study, and therefore, monoterpene concentrations were calculated using  $m/z$  81. For some reason, the monoterpene concentrations were only slightly higher during June–August than during September–May (Table 3), thus, a contribution of other compounds than monoterpenes at  $m/z$  81 might have been possible. On the other hand, Hellén et al. (2012) observed also considerable monoterpene concentrations at the site in winter, spring and fall, possibly due to anthropogenic sources.

Acetone and propanal are both measured at  $m/z$  59 with the PTR-MS but Hellén et al. (2006) showed that the average propanal concentrations are only around 5% compared with the average acetone concentrations in Helsinki during winter. Thus, most of the  $m/z$  59 signal consisted probably of acetone. However, as propanal fluxes at the site are unknown,  $m/z$  59 will still be referred as acetone+propanal.

Measurements at  $m/z$  107 consisted of  $C_2$ -benzenes including, for example, o- and p+m-xylene and ethylbenzene. According to Hellén et al. (2012), major compounds measured at the site is p+m-xylene. Other important compounds reported are o-xylene and ethylbenzene. Hellén et al. (2012) observed annual variation for those compounds with a minima in March. In our study, no considerable differences between June–August and September–May were observed. However, the measured concentrations in this study were quite close to the corresponding values from Hellén et al. (2012). For example, summed concentration of o-, p+m-xylene and ethylbenzene was ca. 0.16 ppb in July (Hellén et al., 2012) whereas in this study, a mean value from June–August was 0.23 ppb (Table 3).

Mass-to-charge ratio 42 is connected with acetonitrile but Dunne et al. (2012) observed the signal might be partly contaminated by product ions formed in reactions with  $NO^+$  and  $O_2^+$  that exist as trace amounts inside the PTR-MS. However, that effect was impossible to quantify in this study, thus,  $m/z$  42 was assumed to consist of acetonitrile.



## 2.3 Estimating biogenic contribution of isoprene

The well-known algorithm for isoprene emissions ( $E_{\text{iso}}$ ) is written as

$$E_{\text{iso}} = E_{0,\text{synth}} C_T C_L, \quad (4)$$

where  $E_{0,\text{synth}}$ ,  $C_T$  and  $C_L$  are the same as in the traditional isoprene algorithm (Guenther et al., 1991, 1993; Guenther, 1997).

- 5 The shape of this algorithm is based on the light response curve of the electron transport activity ( $C_L$ ) and the temperature dependence of the protein activity ( $C_T$ ). The emission potential,  $E_{0,\text{synth}}$ , describes the emission rate of isoprene at  $T = 30^\circ\text{C}$  where  $T$  is the leaf temperature (the ambient temperature in this study).

For other compounds, such as methanol or monoterpenes, no empirical algorithms were applied.

## 3 Results and discussion

### 10 3.1 Observed VOC fluxes and their general behaviour

Significant fluxes were observed for methanol ( $m/z$  33), acetaldehyde ( $m/z$  45), ethanol+formic acid ( $m/z$  47), acetone+propanal ( $m/z$  59), isoprene+furan ( $m/z$  69), benzene ( $m/z$  79), toluene ( $m/z$  93),  $C_2$ -benzenes ( $m/z$  107) and sum of monoterpenes ( $m/z$  81). The fluxes of these compounds had also a diurnal cycle at least in one of the wind sectors (Fig. 3, Table 1). Correlation coefficients between VOC, CO,  $\text{CO}_2$  fluxes and traffic rates are shown in Table A1.

- 15 Methyl *tert*-butyl ether (MTBE) and *tert*-Amyl methyl ether (TAME) are commonly connected to the vehicle exhaust emissions as the compounds were used to increase the octane number of gasoline (e.g. Hellén et al., 2006). MTBE and TAME were measured at their parental ions at  $m/z$  89 and  $m/z$  103, respectively. However, both mass-to-charge ratios showed no significant fluxes, and therefore, those measurements were excluded from further analysis. As the identification of these mass-to-charge ratios was uncertain, both  $m/z$  89 and  $m/z$  103 are marked as *unknown* in Table 2. Formaldehyde, which was measured at  $m/z$  20 31 showed no fluxes either, therefore,  $m/z$  31 was excluded from further analysis as well.

- Fluxes of aromatic compounds (benzene, toluene,  $C_2$ -benzenes) did not show any seasonal variation during the measurement period (Table 3). This was expected because biogenic emissions of these compounds should be either small or negligible and anthropogenic emissions from traffic are unlikely to have considerable seasonal variation. On the other hand, the traffic counts are lower during June–August (Fig. 1) but the average aromatic fluxes had no statistically significant differences between 25 September–May and June–August (Table 3). Nevertheless, benzene and toluene concentrations had a clear annual trend with a minimum during June–August. This is a well understood pattern and is partly caused by the different atmospheric lifetimes between seasons (e.g. Hellén et al., 2012). The ratio of aromatic fluxes to total measured VOC fluxes had also variations as the terpenoid fluxes had a clear seasonal cycle (Fig. 4).

- Methanol, acetone+propanal and acetaldehyde had higher average fluxes during June–August compared with the other 30 months (Table 3). However, the differences were rather small, indicating only minor biogenic emissions compared with the



other sources. The ratio of measured OVOC fluxes to the total measured VOC fluxes stayed stable, being 55–62% in all sectors (Fig. 4).

A clear biogenic signal was observed only for isoprene+furan which had a large difference in both fluxes and concentrations between June–August and September–May (Table 3). Therefore, the fraction of terpenoid fluxes of with all measured VOC  
5 fluxes was also higher in June–August than in September–May (Fig 4). The isoprene+furan flux followed also well the ambient temperature (Fig. 5).

### 3.2 CO fluxes

The CO flux was observed to have a clear diurnal cycle, and as expected, the highest emissions were detected from the road sector (Fig. 6) where the traffic emissions are at their highest. The measured CO fluxes from the road sector also correlated  
10 very well with both corresponding CO<sub>2</sub> fluxes ( $r = 0.69$ ,  $p < 0.001$ ) and traffic rates ( $r = 0.56$ ,  $p < 0.001$ , Fig. 7). The average and median CO and CO<sub>2</sub> fluxes and CO concentrations from April 3 – May 27 2014 are presented in Table 4.

During the measurement period, the average CO flux from the traffic sector was ca. 0.46% compared with the corresponding CO<sub>2</sub> flux. On the other hand, CO<sub>2</sub> had probably already biogenic uptake between April and May 2014 (Järvi et al., 2012; Fig. 6; Table 4). Therefore, a better estimate for the flux ratio was taken from Järvi et al. (2012) who estimated that the CO<sub>2</sub>  
15 emission rate from the road sector is  $264 \mu\text{g m}^{-2}\text{s}^{-1}(1000 \text{ veh h}^{-1})^{-1}$  (based on wintertime data from 5 years). In our study, the corresponding CO emission rate from traffic was  $0.9 \mu\text{g m}^{-2}\text{s}^{-1}(1000 \text{ veh h}^{-1})^{-1}$  which is ca. 0.34% compared with the corresponding emission rate of CO<sub>2</sub> in mass basis. Järvi et al. (2012) used data from a more narrow wind sector, 40–120°. However, average CO fluxes had no considerable differences between more narrow and the whole road sector, thus, this had probably only a minor effect on the results. The CO/CO<sub>2</sub> fraction is smaller than in previous study conducted in Edinburgh by  
20 Famulari et al. (2010) who estimated that the traffic related CO emissions are 0.60% compared with the corresponding CO<sub>2</sub> emissions in Edinburgh (in mass basis). In that study, the CO/CO<sub>2</sub> flux ratio was also otherwise quite large, 1.36%. Conversely, Popa et al. (2014) observed a ratio of 0.26% for CO/CO<sub>2</sub> concentrations (in mass basis) in a tunnel study which is quite close to the flux ratio of our study.

Considerable CO fluxes were also observed from the built sector during afternoons (Fig. 6). Such behaviour was not observed  
25 for CO<sub>2</sub> during the same period (Fig. 7). This may be due to many car engines that are started always in the afternoon (between Monday-Friday) when people are leaving the university campus. Catalytic converters that oxidize CO to CO<sub>2</sub> may not work properly right after starting the engine (e.g. Farrauto and Heck, 1999), leading to the high observed CO emissions. Unfortunately, the CO data set from the built sector was very limited from weekends, therefore, CO fluxes from working days could not be compared with CO fluxes from Saturday and Sunday. However, aromatic VOCs seem to also have a similar behaviour with  
30 increasing values during afternoon from the built sector (Fig. 3) which is somewhat expected as Reimann and Lewis (2007, p. 33) mentions that VOC related "cold start emissions" are becoming more and more important.



### 3.3 VOC emissions from different sources

Measured VOC fluxes were studied from all three sectors to estimate sources for VOCs. Based on an older study at the site by Hellén et al. (2006), traffic should be the most important source for aromatic compounds with for example wood combusting explaining less than 1% of the detected benzene concentrations. However, the study by Hellén et al. (2006) was based on the chemical mass balance receptor model with VOC concentrations. Thus the footprint of their study is larger than in our flux measurement based study.

Major emissions could originate also from biogenic sources, at least in the case of isoprene and monoterpenes (Hellén et al., 2012). Thus, isoprene+furan, monoterpenes, methanol, acetone+propanal and acetaldehyde were analysed from two periods: June–August (assumed growing season) and September–May. The division is somewhat rough as many VOCs are also emitted from biogenic sources between September and May. However, these emissions are smaller than during June–August (Rantala et al., 2015).

Other VOC sources could potentially include wood combusting and solvent use. Industry is also a source for VOCs but no industrial activities were located inside flux footprint areas.

#### 3.3.1 Traffic related emissions

Out of the measured compounds, methanol, acetaldehyde, ethanol, acetone, toluene, benzene, and C<sub>2</sub>-benzenes are ingredients of gasoline (Watson et al., 2001; Niven, 2005; Langford et al., 2009). Therefore, traffic is potentially an important anthropogenic source for these compounds. In addition, many studies have shown traffic related isoprene emissions (Reimann et al., 2000; Borbon et al., 2001; Durana et al., 2006; Hellén et al., 2006, 2012). Hellén et al. (2012) also speculated that some monoterpene emissions could originate from traffic.

In recent VOC flux studies at urban sites, fluxes of some VOCs have correlated with traffic rates but this does not necessarily imply causality (Langford et al., 2009, 2010; Park et al., 2010; Valach et al., 2015). At SMEAR III, traffic has been shown to be the most important source for CO<sub>2</sub> at the road sector (Järvi et al., 2012) and same seems to hold also for CO (Table 4). Therefore, the influence of traffic on the VOC emissions was quantified by studying the measured VOC fluxes from this direction.

The difference between average fluxes from road sector and other sectors was statistically significant (95% confidence intervals) for methanol, isoprene+furan, toluene and C<sub>2</sub>-benzenes. However, benzene fluxes were so close to the detection limit that the differences between the sectors were insignificant. All three studied aromatics (benzene, toluene and C<sub>2</sub>-benzenes) were assumed to have same sources, thus, from now on these compounds are analysed together as an "aromatic flux".

The traffic rates and the aromatic fluxes had a significant correlation ( $r = 0.39$ ,  $p < 0.001$ , measurements between January 2013 and September 2014) from the road sector. The aromatic fluxes correlated even better with the measured CO fluxes ( $r = 0.54$ ,  $p < 0.001$ , measurements between April and May 2014). The significant correlation of aromatic VOC flux with CO flux indicates a common source in incomplete combustion. As these both correlated in also with traffic rates, the traffic is likely to be a major source for aromatics.



To estimate the total emission of the aromatic compounds from traffic, the aromatic fluxes were fitted against the traffic rates. A linear model between traffic rates and CO<sub>2</sub> emissions has been suggested, for example, by Järvi et al. (2012). On the other hand, Langford et al. (2010) and Helfter et al. (2011) proposed an exponential fit for VOC and CO<sub>2</sub> emissions. Helfter et al. (2011) mention many reasons for the exponential relationship, such as an increased fuel consumption at higher traffic rates. However, Järvi et al. (2012) did not observe exponential behaviour between CO<sub>2</sub> fluxes and traffic rates at the site, therefore, a linear model was also used in this study. Additionally, an exponential relationship was tested but it brought no clear benefit compared with the linear model. The linear fit gave  $F_{\text{aro}} = (29 \pm 5) \cdot 10^{-3} \text{Tr} + 7 \pm 9 \text{ ng m}^{-2} \text{s}^{-1}$ , where  $F_{\text{aro}}$  is the flux of the aromatics (unit ng m<sup>-2</sup>s<sup>-1</sup>) and Tr is the traffic rate (veh h<sup>-1</sup>). Based on this model and the traffic rates measured in 2013, the aromatic emission from traffic was estimated to be ca.  $1.2 \pm 0.2 \text{ g m}^{-2} \text{yr}^{-1}$ . This is around 0.01% compared with the corresponding CO<sub>2</sub> emission from the road sector (in mass basis) that was estimated using a linear model provided by Järvi et al. (2012).

Methanol fluxes were also observed to correlate with the traffic rates ( $r = 0.34$ ,  $p < 0.001$ , Sep–May) and CO fluxes ( $r = 0.34$ ,  $p = 0.001$ , Apr–May 2014). On the other hand, according to a linear fit, methanol flux values were still around 20 ng m<sup>-2</sup>s<sup>-1</sup> or higher when the traffic rate was close to zero (Fig. 8) which indicates that methanol had probably also other major sources in the road sector. This is also supported by the fact that average methanol fluxes from weekend and weekdays were almost equal (Fig. 9), although traffic rates are clearly larger during weekdays (Fig. 6). However, we were not able to identify any clear sources except possible biogenic emissions during summer. Langford et al. (2010) found also that the traffic counts were able to explain only a part of the observed methanol fluxes but other methanol sources remained unknown in that study as well.

Other oxygenated hydrocarbon fluxes correlated also with the traffic rates. Ethanol+formic acid fluxes were somewhat noisy and mostly close to the detection limit but the correlation between the measured fluxes and the traffic rates was still significant ( $r = 0.20$ ,  $p < 0.001$ , Jan 2013 – Sep 2014). However, no correlation between ethanol+formic acid and CO fluxes was found. Corresponding correlation coefficients for acetone+propanal were 0.24 ( $p < 0.001$ , traffic) and 0.42 ( $p = 0.005$ , CO). The correlation between acetaldehyde and CO flux was 0.30 ( $p = 0.004$ ) and between acetaldehyde flux and the traffic rates 0.31 ( $p < 0.001$ ). Methanol, acetaldehyde and acetone+propanal fluxes had also considerable correlations with each other, indicating that these compounds had probably similar non-traffic related sources at the road sector. The correlation coefficients between methanol and acetaldehyde fluxes and methanol and acetone+propanal fluxes were 0.44 and 0.37, respectively ( $p < 0.001$ , measurements from Sep–May).

Isoprene+furan fluxes that were measured during September–May had a weak but significant correlation ( $r = 0.24$ ,  $p < 0.001$ ) with the traffic rates (Fig. 8). Moreover, the average isoprene+furan fluxes were also positive during September–May (Table 3) indicating that some isoprene+furan fluxes should originate from anthropogenic sources. A correlation between isoprene+furan fluxes and the traffic rates has been earlier observed by Valach et al. (2015). Thus, the correlation found in this study seems reasonable. A correlation between isoprene+furan and CO fluxes was significant ( $r = 0.37$ ,  $p < 0.001$ ) also indicating a traffic related source.



Monoterpene fluxes had no correlation with the traffic rates during September–May. In summer (Jun–Aug), the correlation coefficient between the monoterpene fluxes and the traffic rates was significant,  $r = 0.26$  ( $p < 0.001$ ), but this might also have been a result of increased biogenic emissions as they have similar kind of diurnal cycle compared with the traffic rates. The biogenic influence would be possible to eliminate by dividing the monoterpene fluxes into different temperature classes, however, the amount of data was too small for that kind of analysis. Thus, possible monoterpene emissions from the traffic remained unknown.

Acetonitrile fluxes had no correlation with the traffic rates. This was expected as the only considerable acetonitrile fluxes were observed from the built sector (Fig. 3).

### 3.3.2 Biogenic emissions

Nordbo et al. (2012a) observed that urban  $\text{CO}_2$  fluxes are clearly dependent on the fraction of vegetated land area in flux footprint. Moreover, Järvi et al. (2012) observed that at our measurement site the vegetation sector is a sink for  $\text{CO}_2$  during summer (see also Fig. 6). Thus, biogenic VOC emissions could be expected at the site. For isoprene+furan, the biogenic contribution was clear, and an anticorrelation ( $r = -0.54$ ,  $p < 0.001$ ) between  $\text{CO}_2$  and isoprene+furan fluxes were observed from the vegetation sector during June–August. Isoprene+furan fluxes were also affected by the ambient temperature with small fluxes at low temperatures (roughly  $T < 10^\circ\text{C}$ , Fig. 5). Also methanol fluxes had a high anticorrelation with carbon dioxide fluxes at vegetation sector between June and August ( $r = -0.61$ ,  $p < 0.001$ ) indicating a biogenic source.

Isoprene+furan fluxes were fitted against the empirical isoprene algorithm (Eq. 4) for each wind direction. It has been shown before that the emission potential of isoprene might have seasonal cycle with maximum during midsummer (e.g. in the case of aspen: Fuentes et al., 1999; see also Rantala et al., 2015). However, due to a lack of data points, the fitting was done for the whole summer period (Jun–Aug) only.

The emission potentials,  $E_{0,\text{synth}}$ , from each wind sector (Jun–Aug) for isoprene+furan are presented in Fig. 10 and Table 5. The potentials are roughly twice as high that has been measured above a pine dominated boreal forest in Hyytiälä, Southern Finland (Rantala et al., 2015), although the fraction of vegetation cover at SMEAR III is only 38–59%. However, this was expected as the urban vegetation consists of mostly broadleaved trees that are major isoprene emitters (e.g. Guenther et al., 2006). The emission potentials from each wind sector were close to each other, especially when considering differences in land use (Tables 1 and 5). In that sense, SMEAR III can be considered as a horizontally homogeneous location from a point of isoprene flux measurements. On the other hand, the algorithm was unable to explain some higher isoprene+furan flux values from the road sector (Fig. 10). These values might be related to random uncertainties but they might also be, for example, a result of traffic related emissions.

Methanol, acetaldehyde and acetone are also emitted from biogenic sources (e.g. Guenther et al., 2012), and the methanol fluxes from the vegetation sector were dependent on the ambient temperature. However, the average methanol flux from the vegetation sector was still around  $30 \text{ ng m}^{-2}\text{s}^{-1}$  when temperature  $T < 10^\circ\text{C}$  which indicates that the biogenic emissions can explain only a minor part of the measured methanol fluxes. For acetaldehyde and acetone+propanal the effect of the ambient temperature was even weaker.



As the biogenic OVOC emissions were difficult to distinguish from other exchange processes, such as traffic related emissions, the biogenic contribution for these compounds was estimated from the average flux values (Table 3). Methanol fluxes were significantly larger during June–August than during September–May, indicating that biogenic sources could explain around 25% of the measured methanol fluxes during June–August (Table 3). This is, of course, only a rough estimate but still reasonable when comparing with, for example, measured biogenic methanol emissions in Hyytiälä, Southern Finland (Rantala et al., 2015). Acetaldehyde and acetone+propanal had also significant differences between the average flux values from June–August and September–May. Those differences were around 20–30% indicating that the possible biogenic contribution for these compounds is quite small even during June–August.

Monoterpene fluxes were highly scattered (Fig. 3) and the fluxes were also clearly above zero when temperature  $T < 10^{\circ}\text{C}$  (Fig. 5) indicating significant monoterpene emissions from other sources than biogenic ones. Therefore, no empirical emission algorithms were fitted against monoterpene fluxes. Nevertheless, in June–August the average monoterpene flux was almost twice as high compared with the average flux from September–May. The monoterpene fluxes were also dependent on the ambient temperature (Fig. 5). Therefore, biogenic contribution during June–August was assumed to be around 40% compared with the total monoterpene emissions.

### 3.3.3 Other VOC sources or sinks

Other potential sources of VOCs, mainly wood combustion and solvent use, were found to be difficult to identify. For example, quite large acetone+propanal emissions were observed from built sector in the afternoon (Fig. 3), and the difference between the weekdays and weekend values was also statistically significant (95% confidence intervals, see Fig. 9). These emissions might have been originating from the chemistry department near the site that uses acetone as a solvent.

Nevertheless, methanol, acetaldehyde and acetone+propanal were observed to have emissions that were independent of both ambient temperature and traffic rates. For methanol, these emissions were around  $20\text{--}45\text{ ng m}^{-2}\text{s}^{-1}$  from the road sector (Fig. 8) which is correspondingly around 30–70 % compared with the average methanol flux (Table 3, Fig. 9). The offset was larger during June–August than during September–May but the difference was statistically insignificant. Recent studies (e.g. Wohlfahrt et al., 2015 and references therein, Rantala et al., 2015; Schallhart et al., 2015) have shown that deposition might have also a significant role in OVOC exchange in some ecosystems. However, no clear signals of net deposition was observed for any of the studied OVOCs. Overall, non-traffic sources were estimated to explain around 50% of the anthropogenic OVOC emissions between September and May.

Globally, aromatic compounds have also other sources than traffic, such as solvent and petroleum use (Na et al., 2005; Srivastava et al., 2005; Langford et al., 2009). When considering an offset of around  $7\text{ ng m}^{-2}\text{s}^{-1}$  of the linear fit between the aromatic fluxes and the traffic rates (Fig. 8), emissions of aromatic compounds from non-traffic sources might have also been possible at the SMEAR III. Nevertheless, an influence of non-traffic sources was rather small.

Isoprene+furan had small emissions around  $2\text{--}5\text{ ng m}^{-2}\text{s}^{-1}$  (Fig. 5 and Table 3) from other sources than biogenic ones. They might be traffic-related as discussed above but they may also originate from petroleum products (Langford et al., 2009). Nevertheless, the contribution of other than biogenic isoprene+furan emissions was small during June–August.



Acetonitrile had significant emissions only from the built sector. This indicates that the major sources of acetonitrile are not traffic related, although Holzinger et al. (2001) found weak traffic related acetonitrile emissions, and Langford et al. (2010) measured acetonitrile fluxes that correlated with the traffic rates. On the other hand, Langford et al. (2010) also mentioned that despite of the correlation, the acetonitrile sources were left unknown. In this study, a possible source for the acetonitrile could have been wood combusting in the residential building area, which is located around 200–400 m from the site, and thus at the edge of the typical flux footprint area (see Ripamonti et al., 2013). However, the acetonitrile fluxes were mostly noisy and below the detection limit, making any final conclusions challenging.

### 3.4 Comparing results to previous VOC studies

Generally, the measured VOC fluxes were much lower than those reported previous urban VOC flux studies (Fig. 11). For example, Velasco et al. (2005) measured an order of magnitude higher methanol, acetone+propanal, toluene and C<sub>2</sub>-benzene fluxes in Mexico City compared with this study. Most of the previous measurements were done in the city centres while this study was done at the urban background site, which likely has a considerable effect on the magnitude of VOC fluxes. For example, Reimann and Lewis (2007, p. 53) mentions that aromatic concentrations were lower in suburban area of Zürich compared with the city centre.

For measured CO<sub>2</sub> fluxes, intercity variations are also found to be considerable (Nordbo et al., 2012a). For example, Helfter et al. (2011) measured ca. five times higher CO<sub>2</sub> fluxes in London than Järvi et al. (2012) at SMEAR III (Fig. 11). The variations in carbon dioxide fluxes can be due to the intensity of the anthropogenic activity, the differences in heating systems (central, electrical, domestic gas, coal, oil or wood fired heating systems), the means of public transport (electric buses and trams or diesel buses) etc. The relatively low VOC fluxes observed in this study are in line with low carbon dioxide flux, both of which indicate relatively low anthropogenic intensity for an urban area. In this study, for example, traffic related aromatic emissions were around 0.01% compared with the corresponding CO<sub>2</sub> emissions, and according to Valach et al. (2015), aromatic VOC fluxes measured in London were around 0.025% compared with the corresponding average CO<sub>2</sub> fluxes (scaled from yearly CO<sub>2</sub> budget, see Helfter et al., 2011). Hence, the VOC flux to CO<sub>2</sub> flux ratio is in the same order of magnitude, although there is almost one order of magnitude difference between the absolute aromatic flux values.

Fraction of urban vegetation has a strong influence on a CO<sub>2</sub> exchange (Nordbo et al., 2012a), thus a perfect correlation between VOC and CO<sub>2</sub> fluxes cannot be expected. However, larger CO<sub>2</sub> fluxes could indicate also larger VOC fluxes as both have common sources, such as traffic. In Figure 11 average urban VOC fluxes reported in literature are plotted against corresponding average CO<sub>2</sub> fluxes. Lowest average VOC and CO<sub>2</sub> fluxes were found in Helsinki (Fig. 11). On the other hand, the largest CO<sub>2</sub> fluxes were measured in London, although the largest VOC fluxes were measured in Mexico City. The large VOC fluxes in Mexico City can be due to much older vehicle fleet, fewer catalytic converters and poorer fuel quality in Mexico City than in UK (Langford et al., 2009).

VOC flux spectrum also differed between the cities (Fig. 11). Benzene was the least emitted compound in all three studies which is an expected result of a development of catalytic converters and changes in fuel composition, traffic related benzene



emission have generally decreased dramatically (Reimann and Lewis, 2007, p. 33 and references therein). Otherwise, the VOC flux spectra seem to be unique for each measurement location.

#### 4 Conclusions

We present results from the first urban VOC flux measurements in a northern city with cold winters. Out of 13 measured mass-to-charge ratios, fluxes were observed for ten. These compounds have been observed to be emitted also in previous urban VOC flux studies reported in literature. The different land use forms in different wind directions enabled us to analyse the different sources of various compounds.

Methanol had the highest fluxes both in June–August and September–May. Other OVOCs, toluene and C<sub>2</sub>-benzenes fluxes were of the same magnitude with each other and had no considerable differences between winter and summer. On the other hand, isoprene+furan fluxes were clearly higher during June–August than during September–May, indicating the major contribution of biogenic isoprene emissions.

All compounds with detectable fluxes had anthropogenic sources at the site. Aromatic compounds originated mostly from traffic whereas for isoprene+furan, the anthropogenic influence was only minor. However, even those small isoprene+furan fluxes can have relatively large influence on isoprene+furan concentrations during winter when the biogenic emission is small. For monoterpenes, the anthropogenic influence was larger, being of similar magnitude with the biogenic emissions in summer. Oxygenated VOCs originated from traffic, vegetation and unknown anthropogenic sources, which probably included solvent use at the University campus. Generally, the magnitude of traffic related OVOC emissions was estimated to be similar to other anthropogenic sources. Biogenic activity had only a minor contribution in the total annual OVOC exchange. For methanol, the biogenic emissions explained up to 25% of the measured flux values during June–August.

Measured VOC fluxes were much lower than has earlier been observed in the urban VOC flux studies. On the other hand, most of the urban VOC flux studies have been carried out in dense city centres, such as in London, whereas this study was done ca. five kilometres from the Helsinki city centre in a semi-urban area. Moreover, also the CO<sub>2</sub> fluxes have been observed to be relatively low at SMEAR III compared with other urban stations. However, the variation of CO<sub>2</sub> flux does not fully explain the variation in the VOC fluxes between different urban areas.

The measured urban VOC fluxes have considerable variations between different locations both in quantity and in quality. Thus a parameterization for a VOC exchange in urban areas may be challenging. However, links between VOC emissions and CO<sub>2</sub> and CO emission provide indication of processes which need to be described by such parameterizations. For this a larger body of concomitant measurements of VOC, CO and CO<sub>2</sub> fluxes may be needed.



## Appendix A

**Table A1.** Correlation coefficients from each wind sector between VOC, CO, CO<sub>2</sub> fluxes and traffic rates (Tr, only from the road sector) using all available data. Insignificant ( $p > 0.05$ ) correlation coefficients are not shown in the Table. For the comparison, the correlation coefficient between CO<sub>2</sub> fluxes and the traffic rates was calculated from the same period with CO fluxes (Apr–May 2014).

Road sector													
	<i>m/z</i> 33	<i>m/z</i> 42	<i>m/z</i> 45	<i>m/z</i> 47	<i>m/z</i> 59	<i>m/z</i> 69	<i>m/z</i> 79	<i>m/z</i> 81	<i>m/z</i> 93	<i>m/z</i> 107	CO	CO <sub>2</sub>	Tr
<i>m/z</i> 33	1	–	0.51	0.31	0.36	0.35	0.27	0.21	0.28	0.34	0.34	0.32	0.32
<i>m/z</i> 42	–	1	–	–	–	0.12	–	–	–	–	–	–	–
<i>m/z</i> 45	0.51	–	1	0.33	0.44	0.45	0.30	0.16	0.34	0.34	0.30	0.31	0.31
<i>m/z</i> 47	0.31	–	0.33	1	0.15	0.10	0.22	0.13	0.22	0.25	–	0.37	0.20
<i>m/z</i> 59	0.36	–	0.44	0.15	1	0.32	0.24	0.22	0.18	0.33	0.42	0.13	0.24
<i>m/z</i> 69	0.35	0.12	0.45	0.10	0.32	1	0.19	0.21	0.22	0.21	0.37	–	0.32
<i>m/z</i> 79	0.27	–	0.30	0.22	0.24	0.19	1	0.08	0.26	0.25	0.43	0.22	0.17
<i>m/z</i> 81	0.21	–	0.16	0.13	0.22	0.21	0.08	1	0.14	0.17	–	0.11	0.15
<i>m/z</i> 93	0.28	–	0.34	0.22	0.18	0.22	0.26	0.14	1	0.36	0.38	0.36	0.30
<i>m/z</i> 107	0.34	–	0.34	0.25	0.33	0.21	0.25	0.17	0.36	1	0.37	0.39	0.34
CO	0.34	–	0.30	–	0.42	0.37	0.43	–	0.38	0.37	1	0.69	0.56
CO <sub>2</sub>	0.32	–	0.31	0.37	0.13	–	0.22	0.11	0.36	0.39	0.69	1	0.58
tr	0.32	–	0.31	0.20	0.24	0.32	0.17	0.15	0.30	0.34	0.56	0.58	1
Vegetation sector													
	<i>m/z</i> 33	<i>m/z</i> 42	<i>m/z</i> 45	<i>m/z</i> 47	<i>m/z</i> 59	<i>m/z</i> 69	<i>m/z</i> 79	<i>m/z</i> 81	<i>m/z</i> 93	<i>m/z</i> 107	CO	CO <sub>2</sub>	
<i>m/z</i> 33	1	0.12	0.55	0.31	0.43	0.35	0.17	0.21	0.26	0.23	0.36	-0.29	
<i>m/z</i> 42	0.12	1	0.10	0.07	0.12	–	–	–	0.12	0.10	–	–	
<i>m/z</i> 45	0.55	0.10	1	0.36	0.41	0.35	0.12	0.14	0.20	0.19	0.33	-0.14	
<i>m/z</i> 47	0.31	0.07	0.36	1	0.24	–	0.20	0.10	0.17	0.22	0.18	0.14	
<i>m/z</i> 59	0.43	0.12	0.41	0.24	1	0.25	0.18	0.11	0.25	0.19	0.38	-0.11	
<i>m/z</i> 69	0.35	–	0.35	–	0.25	1	0.08	0.11	0.11	0.17	–	-0.43	
<i>m/z</i> 79	0.17	–	0.12	0.20	0.18	0.08	1	0.07	0.15	0.13	0.21	–	
<i>m/z</i> 81	0.21	–	0.14	0.10	0.11	0.11	0.07	1	0.13	–	–	-0.17	
<i>m/z</i> 93	0.26	0.12	0.20	0.17	0.25	0.11	0.15	0.13	1	0.18	0.28	–	
<i>m/z</i> 107	0.23	0.10	0.19	0.22	0.19	0.17	0.13	–	0.18	1	0.27	0.08	
CO	0.36	–	0.33	0.18	0.38	–	0.21	–	0.28	0.27	1	0.26	
CO <sub>2</sub>	-0.29	–	-0.14	0.14	-0.11	-0.43	–	-0.17	–	0.08	0.26	1	
Built sector													
	<i>m/z</i> 33	<i>m/z</i> 42	<i>m/z</i> 45	<i>m/z</i> 47	<i>m/z</i> 59	<i>m/z</i> 69	<i>m/z</i> 79	<i>m/z</i> 81	<i>m/z</i> 93	<i>m/z</i> 107	CO	CO <sub>2</sub>	
<i>m/z</i> 33	1	0.24	0.50	0.42	0.38	0.27	0.27	0.19	0.39	0.14	0.33	–	
<i>m/z</i> 42	0.24	1	0.28	0.16	0.31	–	–	0.11	0.20	0.18	0.30	–	
<i>m/z</i> 45	0.50	0.28	1	0.47	0.27	0.21	0.27	0.15	0.29	0.12	–	–	
<i>m/z</i> 47	0.42	0.16	0.47	1	0.22	0.13	0.35	0.14	0.33	0.27	0.38	0.14	
<i>m/z</i> 59	0.38	0.31	0.27	0.22	1	0.25	0.25	0.12	0.37	0.19	0.49	–	
<i>m/z</i> 69	0.27	–	0.21	0.13	0.25	1	0.18	–	0.30	0.17	–	-0.16	
<i>m/z</i> 79	0.27	–	0.27	0.35	0.25	0.18	1	0.10	0.23	0.17	–	–	
<i>m/z</i> 81	0.19	0.11	0.15	0.14	0.12	–	0.10	1	0.14	–	–	–	
<i>m/z</i> 93	0.39	0.20	0.29	0.33	0.37	0.30	0.23	0.14	1	0.29	–	0.14	
<i>m/z</i> 107	0.14	0.18	0.12	0.27	0.19	0.17	0.17	–	0.29	1	–	0.12	
CO	0.33	0.30	–	0.38	0.49	–	–	–	–	–	1	0.42	
CO <sub>2</sub>	–	–	–	0.14	–	-0.16	–	–	0.14	0.12	0.42	1	



*Acknowledgements.* We acknowledge the support from the Doctoral programme of atmospheric sciences, and from the Academy of Finland (ICOS-Finland 281255 and ICOS-ERIC 281250), and from the Academy of Finland through its Centre of Excellence program (Project No 272041 and 125238). We also thank Alessandro Franchin, Sigfried Schoesberger, Simon Schallhart and Lauri Ahonen for their help in carrying the PTR-MS between our laboratory and the measurement site. Finally, we thank all people who made the ancillary data available.



## References

- Ammann, C., Brunner, A., Spirig, C., and Neftel, A.: Technical note: Water vapour concentration and flux measurements with PTR-MS, *Atmospheric Chemistry and Physics*, 6, 4643–4651, 2006.
- Atkinson, R.: Atmospheric chemistry of VOCs and NO<sub>x</sub>, *Atmospheric Environment*, 34, 2063–2101, 2000.
- 5 Atkinson, R. and Arey, J.: Gas-phase tropospheric chemistry of biogenic volatile organic compounds: a review, *Atmospheric Environment*, 37, Supplement 2, 197 – 219, 2003.
- Aubinet, M., Vesala, T., and Papale, D.: *Eddy Covariance: A Practical Guide to Measurement and Data Analysis*, Springer Atmospheric Sciences, Netherlands, 2012.
- Borbon, A., Fontaine, H., Veillerot, M., Locoge, N., Galloo, J., and Guillermo, R.: An investigation into the traffic-related fraction of isoprene  
10 at an urban location, *Atmospheric Environment*, 35, 3749–3760, 2001.
- Borbon, A., Gilman, J. B., Kuster, W. C., Grand, N., Chevaillier, S., Colomb, A., Dolgorouky, C., Gros, V., Lopez, M., Sarda-Esteve, R., Holloway, J., Stutz, J., Petetin, H., McKeen, S., Beekmann, M., Warneke, C., Parrish, D. D., and de Gouw, J. A.: Emission ratios of anthropogenic volatile organic compounds in northern mid-latitude megacities: Observations versus emission inventories in Los Angeles and Paris, *Journal of Geophysical Research: Atmospheres*, 118, 2041–2057, 2013.
- 15 Calfapietra, C., Fares, S., Manes, F., Morani, A., Sgrigna, G., and Loreto, F.: Role of Biogenic Volatile Organic Compounds (BVOC) emitted by urban trees on ozone concentration in cities: A review, *Environmental Pollution*, 183, 71–80, 2013.
- de Gouw, J. and Warneke, C.: Measurements of volatile organic compounds in the earth's atmosphere using proton-transfer-reaction mass spectrometry, *Mass Spectrometry Reviews*, 26, 223–257, 2007.
- Drebs, A., Nordlund, A., Karlsson, P., Helminen, J., and Rissanen, P.: *Tilastoja Suomen ilmastosta 1971–2000 [Climatological statistics of  
20 Finland 1971–2000]*, Finnish Meteorological Institute, Helsinki, 2002.
- Dunne, E., Galbally, I. E., S. L., and Patti, A.: Interference in the PTR-MS measurement of acetonitrile at  $m/z$  42 in polluted urban air – A study using switchable reagent ion PTR-MS, *Int. J. Mass Spectrom.*, 319–320, 40–47, 2012.
- Durana, N., Navazo, M., Gomez, M., Alonso, L., García, J., Iardía, J., Gangoiti, G., and Iza, J.: Long term hourly measurement of 62 non-methane hydrocarbons in an urban area: Main results and contribution of non-traffic sources, *Atmospheric Environment*, 40, 2860–2872,  
25 2006.
- Famulari, D., Nemitz, E., Marco, C. D., Phillips, G. J., Thomas, R., House, E., and Fowler, D.: Eddy-covariance measurements of nitrous oxide fluxes above a city, *Agricultural and Forest Meteorology*, 150, 786–793, 2010.
- Farrauto, R. J. and Heck, R. M.: Catalytic converters: state of the art and perspectives, *Catalysis Today*, 51, 351–360, 1999.
- Filella, I. and Peñuelas, J.: Daily, weekly, and seasonal time courses of VOC concentrations in a semi-urban area near Barcelona, *Atmospheric  
30 Environment*, 40, 7752–7769, 2006.
- Foken, T. and Wichura, B.: Tools for quality assessment of surface-based flux measurements, *Agricultural and Forest Meteorology*, 78, 83–105, 1996.
- Fuentes, J. D., Wang, D., and Gu, L.: Seasonal Variations in Isoprene Emissions from a Boreal Aspen Forest, *Journal of Applied Meteorology*, 38, 855–869, 1999.
- 35 Guenther, A. B.: Seasonal and spatial variations in natural volatile organic compound emissions, *Ecological Applications*, 7, 34–45, 1997.
- Guenther, A. B., Monson, R. K., and Fall, R.: Isoprene and Monoterpene Emission Rate Variability: Observations With Eucalyptus and Emission Rate Algorithm Development, *Journal of Geophysical Research*, 96, 10 799–10 808, 1991.



- Guenther, A. B., Zimmerman, P. R., Harley, P. C., Monson, R. K., and Fall, R.: Isoprene and Monoterpene Emission Rate Variability: Model Evaluations and Sensitivity Analyses, *Journal of Geophysical Research*, 98, 12 609–12 617, 1993.
- Guenther, A. B., Karl, T., Harley, P., Wiedinmyer, C., Palmer, P. I., and Geron, C.: Estimates of global terrestrial isoprene emissions using MEGAN (Model of Emissions of Gases and Aerosols from Nature), *Atmospheric Chemistry and Physics*, 6, 3181–3210, doi:10.5194/acp-6-3181-2006, <http://www.atmos-chem-phys.net/6/3181/2006/>, 2006.
- 5 Guenther, A. B., Jiang, X., Heald, C. L., Sakulyanontvittay, T., Duhl, T., Emmons, L., and Wang, X.: The Model of Emissions of Gases and Aerosols from Nature version 2.1 (MEGAN2.1): An extended and updated framework for modeling biogenic emissions, *Geoscientific Model Development*, 5, 1471–1492, doi:10.5194/gmd-5-1471-2012, 2012.
- Helfter, C., Famulari, D., Phillips, G. J., Barlow, J. F., Wood, C. R., Grimmond, C. S. B., and Nemitz, E.: Controls of carbon dioxide concentrations and fluxes above central London, *Atmospheric Chemistry and Physics*, 11, 1913–1928, doi:10.5194/acp-11-1913-2011, <http://www.atmos-chem-phys.net/11/1913/2011/>, 2011.
- 10 Hellén, H., Hakola, H., and Laurila, T.: Determination of source contributions of NMHCs in Helsinki (60°N, 25°E) using chemical mass balance and the Unmix multivariate receptor models, *Atmospheric Environment*, 37, 1413–1424, 2003.
- Hellén, H., Hakola, H., Pirjola, L., Laurila, T., and Pystynen, K.-H.: Ambient air concentrations, source profiles, and source apportionment of 71 different C2-C10 volatile organic compounds in urban and residential areas of Finland, *Environmental science & technology*, 40, 103–108, 2006.
- 15 Hellén, H., Tykkä, T., and Hakola, H.: Importance of monoterpenes and isoprene in urban air in northern Europe, *Atmospheric Environment*, 59, 59–66, 2012.
- Holzinger, R., Jordan, A., Hansel, A., and Lindinger, W.: Automobile Emissions of Acetonitrile: Assessment of its Contribution to the Global Source, *Journal of Atmospheric Chemistry*, 38, 187–193, 2001.
- 20 Horst, T. W.: A simple formula for attenuation of eddy fluxes measured with first-order-response scalar sensors, *Boundary-Layer Meteorology*, 82, 219–233, 1997.
- Ibrom, A., Dellwik, E., Larsen, S. E., and Pilegaard, K.: On the use of the Webb–Pearman–Leuning theory for closed-path eddy correlation measurements, *Tellus B*, 59, 937–946, 2007.
- 25 Järvi, L., Hannuniemi, H., Hussein, T., Junninen, H., Aalto, P. P., Hillamo, R., Mäkelä, T., Keronen, P., Siivola, E., Vesala, T., and Kulmala, M.: The urban measurement station SMEAR III: Continuous monitoring of air pollution and surface-atmosphere interactions in Helsinki, Finland, *Boreal environment research*, 14, 86–109, 2009a.
- Järvi, L., Mammarella, I., Eugster, W., Ibrom, A., Siivola, E., Dellwik, E., Keronen, P., Burba, G., and Vesala, T.: Comparison of net CO<sub>2</sub> fluxes measured with open-and closed-path infrared gas analyzers in an urban complex environment, *Boreal Environment Research*, 14, 499–514, 2009b.
- 30 Järvi, L., Nordbo, A., Junninen, H., Riikonen, A., Moilanen, J., Nikinmaa, E., and Vesala, T.: Seasonal and annual variation of carbon dioxide surface fluxes in Helsinki, Finland, in 2006–2010, *Atmospheric Chemistry and Physics*, 12, 8475–8489, doi:10.5194/acp-12-8475-2012, <http://www.atmos-chem-phys.net/12/8475/2012/>, 2012.
- Järvi, L., Grimmond, C., Taka, M., Nordbo, A., Setälä, H., and Strachan, I.: Development of the Surface Urban Energy and Water Balance Scheme (SUEWS) for cold climate cities, *Geoscientific Model Development*, 7, 1691–1711, 2014.
- 35 Kajos, M. K., Rantala, P., Hill, M., Hellén, H., Aalto, J., Patokoski, J., Taipale, R., Hoerger, C. C., Reimann, S., Ruuskanen, T. M., Rinne, J., and Petäjä, T.: Ambient measurements of aromatic and oxidized VOCs by PTR-MS and GC-MS: intercomparison between



- four instruments in a boreal forest in Finland, *Atmospheric Measurement Techniques*, 8, 4453–4473, doi:10.5194/amt-8-4453-2015, <http://www.atmos-meas-tech.net/8/4453/2015/>, 2015.
- Kansal, A.: Sources and reactivity of NMHCs and VOCs in the atmosphere: A review, *Journal of Hazardous Materials*, 166, 17–26, 2009.
- Karl, T., Spirig, C., Rinne, J., Stroud, C., Prevost, P., Greenberg, J., Fall, R., and Guenther, A.: Virtual disjunct eddy covariance measurements of organic compound fluxes from a subalpine forest using proton transfer reaction mass spectrometry, *Atmospheric Chemistry and Physics*, 2, 279–291, 2002.
- Karl, T., Hansel, A., Cappellin, L., Kaser, L., Herdinger-Blatt, I., and Jud, W.: Selective measurements of isoprene and 2-methyl-3-buten-2-ol based on  $\text{NO}^+$  ionization mass spectrometry, *Atmospheric Chemistry and Physics*, 12, 11 877–11 884, doi:10.5194/acp-12-11877-2012, <http://www.atmos-chem-phys.net/12/11877/2012/>, 2012.
- 10 Kazil, J., Stier, P., Zhang, K., Quaas, J., Kinne, S., O'Donnell, D., Rast, S., Esch, M., Ferrachat, S., Lohmann, U., and Feichter, J.: Aerosol nucleation and its role for clouds and Earth's radiative forcing in the aerosol-climate model ECHAM5-HAM, *Atmospheric Chemistry and Physics*, 10, 10 733–10 752, doi:10.5194/acp-10-10733-2010, <http://www.atmos-chem-phys.net/10/10733/2010/>, 2010.
- Kulmala, M., Suni, T., Lehtinen, K. E. J., Dal Maso, M., Boy, M., Reissell, A., Rannik, U., Aalto, P., Keronen, P., Hakola, H., Bäck, J., Hoffmann, T., Vesala, T., and Hari, P.: A new feedback mechanism linking forests, aerosols, and climate, *Atmospheric Chemistry and Physics*, 4, 557–562, doi:10.5194/acp-4-557-2004, <http://www.atmos-chem-phys.net/4/557/2004/>, 2004.
- 15 Langford, B., Davison, B., Nemitz, E., and Hewitt, C. N.: Mixing ratios and eddy covariance flux measurements of volatile organic compounds from an urban canopy (Manchester, UK), *Atmospheric Chemistry and Physics*, 9, 1971–1987, doi:10.5194/acp-9-1971-2009, <http://www.atmos-chem-phys.net/9/1971/2009/>, 2009.
- Langford, B., Nemitz, E., House, E., Phillips, G. J., Famulari, D., Davison, B., Hopkins, J. R., Lewis, A. C., and Hewitt, C. N.: Fluxes and concentrations of volatile organic compounds above central London, UK, *Atmospheric Chemistry and Physics*, 10, 627–645, doi:10.5194/acp-10-627-2010, <http://www.atmos-chem-phys.net/10/627/2010/>, 2010.
- Langford, B., Acton, W., Ammann, C., Valach, A., and Nemitz, E.: Eddy-covariance data with low signal-to-noise ratio: time-lag determination, uncertainties and limit of detection, *Atmospheric Measurement Techniques*, 8, 4197–4213, doi:10.5194/amt-8-4197-2015, <http://www.atmos-meas-tech.net/8/4197/2015/>, 2015.
- 25 Lilleberg, I. and Hellman, T.: Liikenteen kehitys Helsingissä vuonna 2011, Helsinki City Planning Department 2011, 2011.
- Lindinger, W., Hansel, A., and Jordan, A.: On-line monitoring of volatile organic compounds at pptv levels by means of Proton-Transfer-Reaction Mass Spectrometry (PTR-MS)—Medical applications, food control and environmental research, *International Journal of Mass Spectrometry*, 173, 191–241, 1998.
- Mammarella, I., Launiainen, S., Grönholm, T., Keronen, P., Pumpanen, J., Rannik, Ü., and Vesala, T.: Relative Humidity Effect on the High-Frequency Attenuation of Water Vapor Flux Measured by a Closed-Path Eddy Covariance System, *Journal of Atmospheric and Oceanic Technology*, 26, 1856–1866, 2009.
- Mammarella, I., Peltola, O., Nordbo, A., Järvi, L., and Rannik, U.: EddyUH: an advanced software package for eddy covariance flux calculation for a wide range of instrumentation and ecosystems, Submitted to *Atmos. Meas. Tech. Discus.*, 2015.
- Moore, C. J.: Frequency Response Corrections for Eddy Correlation Systems, *Boundary-Layer Meteorology*, 37, 17–35, 1986.
- 35 Na, K., Moon, K.-C., and Kim, Y. P.: Source contribution to aromatic VOC concentration and ozone formation potential in the atmosphere of Seoul, *Atmospheric Environment*, 39, 5517–5524, 2005.
- Niven, R. K.: Ethanol in gasoline: environmental impacts and sustainability review article, *Renewable and Sustainable Energy Reviews*, 9, 535–555, 2005.



- Nordbo, A., Järvi, L., Haapanala, S., Wood, C. R., and Vesala, T.: Fraction of natural area as main predictor of net CO<sub>2</sub> emissions from cities, *Geophysical Research Letters*, 39, 2012a.
- Nordbo, A., Järvi, L., and Vesala, T.: Revised eddy covariance flux calculation methodologies — effect on urban energy balance, *Tellus B*, 64, 2012b.
- 5 Nordbo, A., Kekäläinen, P., Siivola, E., Lehto, R., Vesala, T., and Timonen, J.: Tube transport of water vapor with condensation and desorption, *Applied Physics Letters*, 102, 2013.
- Nordbo, A., Kekäläinen, P., Siivola, E., Mammarella, I., Timonen, J., and Vesala, T.: Sorption-Caused Attenuation and Delay of Water Vapor Signals in Eddy-Covariance Sampling Tubes and Filters, *Journal of Atmospheric and Oceanic Technology*, 31, 2629–2649, 2014.
- Paasonen, P., Asmi, A., Petäjä, T., Kajos, M. K., Äijälä, M., Junninen, H., Holst, T., Abbatt, J. P. D., Arneth, A., Birmili, W., van der Gon,  
10 H. A. C. D., Hamed, A., Hoffer, A., Laakso, L., Laaksonen, A., Leaitch, W. R., Plass-Dülmer, C., C., P. S., Räisänen, P., Swietlicki, E., Wiedensohler, A., Worsnop, D. R., Kerminen, V.-M., and Kulmala, M.: Warming-induced increase in aerosol number concentration likely to moderate climate change, *Nature Geoscience Letters*, 12, 438–442, 2013.
- Park, C., Schade, G. W., and Boedeker, I.: Flux measurements of volatile organic compounds by the relaxed eddy accumulation method combined with a GC-FID system in urban Houston, Texas, *Atmospheric Environment*, 44, 2605–2614, 2010.
- 15 Park, J.-H., Goldstein, A. H., Timkovsky, J., Fares, S., Weber, R., Karlik, J., and Holzinger, R.: Eddy covariance emission and deposition flux measurements using proton transfer reaction – time of flight – mass spectrometry (PTR-TOF-MS): comparison with PTR-MS measured vertical gradients and fluxes, *Atmospheric Chemistry and Physics*, 13, 1439–1456, doi:10.5194/acp-13-1439-2013, <http://www.atmos-chem-phys.net/13/1439/2013/>, 2013.
- Patokoski, J., Ruuskanen, T. M., Hellén, H., Taipale, R., Grönholm, T., Kajos, M. K., Petäjä, T., Hakola, H., Kulmala, M., and Rinne, J.:  
20 Winter to spring transition and diurnal variation of vocs in Finland at an urban background site and a rural site., *Boreal Environment Research*, 19, 79–103, 2014.
- Patokoski, J., Ruuskanen, T. M., Kajos, M. K., Taipale, R., Rantala, P., Aalto, J., Ryyppö, T., Nieminen, T., Hakola, H., and Rinne, J.: Sources of long-lived atmospheric VOCs at the rural boreal forest site, SMEAR II, *Atmospheric Chemistry and Physics Discussions*, 15, 14593–14641, doi:10.5194/acpd-15-14593-2015, <http://www.atmos-chem-phys-discuss.net/15/14593/2015/>, 2015.
- 25 Popa, M. E., Vollmer, M. K., Jordan, A., Brand, W. A., Pathirana, S. L., Rothe, M., and Röckmann, T.: Vehicle emissions of greenhouse gases and related tracers from a tunnel study: CO : CO<sub>2</sub>, N<sub>2</sub>O : CO<sub>2</sub>, CH<sub>4</sub> : CO<sub>2</sub>, O<sub>2</sub> : CO<sub>2</sub> ratios, and the stable isotopes <sup>13</sup>C and <sup>18</sup>O in CO<sub>2</sub> and CO, *Atmospheric Chemistry and Physics*, 14, 2105–2123, doi:10.5194/acp-14-2105-2014, <http://www.atmos-chem-phys.net/14/2105/2014/>, 2014.
- Rannik, Ü. and Vesala, T.: Autoregressive filtering versus linear detrending in estimation of fluxes by the eddy covariance method, *Boundary-  
30 Layer Meteorology*, 91, 259–280, 1999.
- Rantala, P., Taipale, R., Aalto, J., Kajos, M. K., Patokoski, J., Ruuskanen, T. M., and Rinne, J.: Continuous flux measurements of VOCs using PTR-MS —reliability and feasibility of disjunct-eddy-covariance, surface-layer-gradient, and surface-layer-profile methods, *Boreal Environment Research*, 19B, 87–107, 2014.
- Rantala, P., Aalto, J., Taipale, R., Ruuskanen, T. M., and Rinne, J.: Annual cycle of volatile organic compound exchange between a boreal pine  
35 forest and the atmosphere, *Biogeosciences*, 12, 5753–5770, doi:10.5194/bg-12-5753-2015, <http://www.biogeosciences.net/12/5753/2015/>, 2015.
- Reimann, S. and Lewis, A. C.: Anthropogenic VOCs, in: *Volatile Organic Compounds in the Atmosphere*, edited by Koppman, R., chap. 2, Blackwell Publishing Ltd, Oxford, 2007.



- Reimann, S., Calanca, P., and Hofer, P.: The anthropogenic contribution to isoprene concentrations in a rural atmosphere, *Atmospheric Environment*, 34, 109–115, 2000.
- Rinne, J. and Amman, C.: Disjunct Eddy Covariance Method, in: *Eddy Covariance: A Practical Guide to Measurement and Data Analysis*, edited by Aubinet, M., Vesala, T., and Papale, D., chap. 10, Springer, New York, 2012.
- 5 Rinne, J., Guenther, A. B., Warneke, C., de Gouw, J. A., and Luxembourg, S. L.: Disjunct eddy covariance technique for trace gas flux measurements, *Geophysical Research Letters*, 28, 3139–3142, 2001.
- Rinne, J., Markkanen, T., Ruuskanen, T. M., Petäjä, T., Keronen, P., Tang, M. J., Crowley, J. N., Rannik, Ü., and Vesala, T.: Effect of chemical degradation on fluxes of reactive compounds – a study with a stochastic Lagrangian transport model, *Atmospheric Chemistry and Physics*, 12, 4843–4854, 2012.
- 10 Ripamonti, G., Järvi, L., Mølgaard, B., Hussein, T., Nordbo, A., and Hämeri, K.: The effect of local sources on aerosol particle number size distribution, concentrations and fluxes in Helsinki, Finland, *Tellus B*, 65, 2013.
- Schallhart, S., Rantala, P., Nemitz, E., Mogensen, D., Tillmann, R., Mentel, T. F., Rinne, J., and Ruuskanen, T. M.: Characterization of total ecosystem scale biogenic VOC exchange at a Mediterranean oak-hornbeam forest, *Atmospheric Chemistry and Physics Discussions*, 15, 27 627–27 673, doi:10.5194/acpd-15-27627-2015, <http://www.atmos-chem-phys-discuss.net/15/27627/2015/>, 2015.
- 15 Spracklen, D. V., Bonn, B., and Carslaw, K. S.: Boreal forests, aerosols and the impacts on clouds and climate, *Philosophical Transactions of the Royal Society of London A: Mathematical, Physical and Engineering Sciences*, 366, 4613–4626, doi:10.1098/rsta.2008.0201, 2008.
- Srivastava, A., Joseph, A., More, A., and Patil, S.: Emissions of VOCs at Urban Petrol Retail Distribution Centres in India (Delhi and Mumbai), *Environmental Monitoring and Assessment*, 109, 227–242, 2005.
- Stewart, I. D. and Oke, T. R.: Local climate zones for urban temperature studies, *Bulletin of the American Meteorological Society*, 93, 1879–1900, 2012.
- 20 Taipale, R., Ruuskanen, T. M., Rinne, J., Kajos, M. K., Hakola, H., Pohja, T., and Kulmala, M.: Technical Note: Quantitative long-term measurements of VOC concentrations by PTR-MS — measurement, calibration, and volume mixing ratio calculation methods, *Atmospheric Chemistry and Physics*, 8, 6681–6698, doi:10.5194/acp-8-6681-2008, <http://www.atmos-chem-phys.net/8/6681/2008/>, 2008.
- Taipale, R., Ruuskanen, T. M., and Rinne, J.: Lag time determination in DEC measurements with PTR-MS, *Atmospheric Measurement Techniques*, 3, 853–862, doi:10.5194/amt-3-853-2010, <http://www.atmos-meas-tech.net/3/853/2010/>, 2010.
- 25 Tani, A., Hayward, S., and Hewitt, C.: Measurement of monoterpenes and related compounds by proton transfer reaction-mass spectrometry (PTR-MS), *International Journal of Mass Spectrometry*, 223–224, 561–578, 2003.
- Valach, A. C., Langford, B., Nemitz, E., MacKenzie, A. R., and Hewitt, C. N.: Seasonal and diurnal trends in concentrations and fluxes of volatile organic compounds in central London, *Atmospheric Chemistry and Physics*, 15, 7777–7796, doi:10.5194/acp-15-7777-2015, <http://www.atmos-chem-phys.net/15/7777/2015/>, 2015.
- 30 Velasco, E., Lamb, B., Pressley, S., Allwine, E., Westberg, H., Jobson, B. T., Alexander, M., Prazeller, P., Molina, L., and Molina, M.: Flux measurements of volatile organic compounds from an urban landscape, *Geophysical Research Letters*, 32, 2005.
- Velasco, E., Pressley, S., Grivicke, R., Allwine, E., Coons, T., Foster, W., Jobson, B. T., Westberg, H., Ramos, R., Hernández, F., Molina, L. T., and Lamb, B.: Eddy covariance flux measurements of pollutant gases in urban Mexico City, *Atmospheric Chemistry and Physics*, 9, 7325–7342, doi:10.5194/acp-9-7325-2009, <http://www.atmos-chem-phys.net/9/7325/2009/>, 2009.
- 35 Vesala, T., Järvi, L., Launiainen, S., Sogachev, A., Rannik, U., Mammarella, I., Siivola, E., Keronen, P., Rinne, J., Riikonen, A., and Nikinmaa, E.: Surface–atmosphere interactions over complex urban terrain in Helsinki, Finland, *Tellus B*, 60, 188–199, 2008.



Watson, J. G., Chow, J. C., and Fujita, E. M.: Review of volatile organic compound source apportionment by chemical mass balance, *Atmospheric Environment*, 35, 1567–1584, 2001.

5 Wohlfahrt, G., Amelynck, C., Ammann, C., Arneth, A., Bamberger, I., Goldstein, A. H., Gu, L., Guenther, A., Hansel, A., Heinesch, B., Holst, T., Hörtnagl, L., Karl, T., Laffineur, Q., Neftel, A., McKinney, K., Munger, J. W., Pallardy, S. G., Schade, G. W., Seco, R., and Schoon, N.: An ecosystem-scale perspective of the net land methanol flux: synthesis of micrometeorological flux measurements, *Atmospheric Chemistry and Physics*, 15, 7413–7427, doi:10.5194/acp-15-7413-2015, <http://www.atmos-chem-phys.net/15/7413/2015/>, 2015.



**Table 1.** The table presents three sectors around the measurement site and the fraction of vegetation of each sector ( $f_x$ , see Järvi et al., 2014). The average CO<sub>2</sub> flux values (in carbon basis) were taken from Järvi et al. (2012).

	$f_{\text{paved}}$	$f_{\text{build}}$	$f_{\text{veg}}$	Annual CO <sub>2</sub> emissions [gC m <sup>-2</sup> ] (five-year average)
All	0.36	0.15	0.49	1760
Built (320–40°)	0.42	0.20	0.38	
Road (40–180°)	0.39	0.15	0.46	3500
Vegetation (180–320°)	0.30	0.11	0.59	870



**Table 2.** The compound names and the formulas listed below in third and fourth column, respectively, are estimates for the measured mass-to-charge ratios (see e.g. de Gouw and Warneke, 2007). The second column shows whether a sensitivity was determined directly from the calibration or from a transmission curve (i.e. *calculated*), and which compounds were used in the calibrations. *m/z* 89 and *m/z* 103 were measured only during 27.6.–27.8.2014. Due to software problems, some data were lost. Those gaps are marked by superscripts *a* and *b* that correspond to the lost periods 27 June–9 July 2014 and 27 August–30 September, respectively. The final column shows data coverages (flux values) for each compound from the whole period January 2013–September 2014.

[ <i>m/z</i> ]	Calibration compound	Compound	Chemical formula	Data coverage [%]
31 <sup>a</sup>	<i>calculated</i>	formaldehyde	CH <sub>2</sub> O	–
33 <sup>a</sup>	methanol	methanol	CH <sub>4</sub> O	32.2
42 <sup>a</sup>	acetonitrile	acetonitrile, alkane products	C <sub>2</sub> H <sub>3</sub> N	32.4
45 <sup>a</sup>	acetaldehyde	acetaldehyde	C <sub>2</sub> H <sub>4</sub> O	32.6
47 <sup>a</sup>	<i>calculated</i>	ethanol, formic acid	C <sub>2</sub> H <sub>6</sub> O, CH <sub>2</sub> O <sub>2</sub>	32.9
59 <sup>a</sup>	acetone	acetone, propanal	C <sub>3</sub> H <sub>6</sub> O	37.0
69 <sup>a</sup>	isoprene	isoprene, furan	C <sub>5</sub> H <sub>8</sub>	32.1
79 <sup>b</sup>	benzene	benzene	C <sub>6</sub> H <sub>6</sub>	32.8
81 <sup>b</sup>	α-pinene	monoterpene fragments		28.5
89 <sup>b</sup>	<i>calculated</i>	<i>unknown</i>	–	–
93 <sup>b</sup>	toluene	toluene	C <sub>7</sub> H <sub>8</sub>	31.7
103 <sup>b</sup>	<i>calculated</i>	<i>unknown</i>	–	–
107 <sup>b</sup>	m-xylene,o-xylene	C <sub>2</sub> -benzenes	C <sub>8</sub> H <sub>10</sub>	30.9
137 <sup>b</sup>	α-pinene	monoterpenes	C <sub>10</sub> H <sub>16</sub>	–



**Table 3.** Average and median fluxes for each measured VOC compound excluding  $m/z$  31,  $m/z$  89 and  $m/z$  103. Error estimates of the average values were calculated using the equation  $1.96 \cdot \sigma_{\text{VOC}} / \sqrt{N}$ , where  $\sigma_{\text{VOC}}$  is the standard deviation of a VOC time series and  $N$  the number of data points. Lower and upper quartiles are given in parenthesis after the median values. A percentage of the lowest and highest values were disregarded from the time series to avoid effect of possible outliers.

	$m/z$ 33	$m/z$ 42	$m/z$ 45	$m/z$ 47	$m/z$ 59	$m/z$ 69	$m/z$ 79	$m/z$ 81	$m/z$ 93	$m/z$ 107
VOC flux [ $\text{ng m}^{-2} \text{s}^{-1}$ ]										
<b>Jan 2013–Sep 2014</b>										
mean	44.9 ( $\pm 2.5$ )	0.7 ( $\pm 0.1$ )	10.1 ( $\pm 0.6$ )	22.0 ( $\pm 1.7$ )	16.6 ( $\pm 1.1$ )	8.1 ( $\pm 0.6$ )	5.5 ( $\pm 0.6$ )	10.9 ( $\pm 1.2$ )	14.1 ( $\pm 1.1$ )	16.4 ( $\pm 1.4$ )
median	29.4 (10.4...62.1)	0.7 (-1.2...2.2)	8.3 (2.4...16.7)	16.6 (-0.8...35.3)	11.6 (2.1...25.8)	5.5 (-0.6...14.1)	4.6 (-2.2...11.2)	11.0 (-5.7...25.6)	11.4 (-1.3...26)	14.6 (-3.7...33)
$N$	2023	2036	2052	2068	2313	2020	2092	1822	2031	1985
<b>Jun–Aug</b>										
mean	54.2 ( $\pm 4.5$ )	0.6 ( $\pm 0.2$ )	11.8 ( $\pm 1$ )	14.7 ( $\pm 2.2$ )	20.6 ( $\pm 2.1$ )	14.3 ( $\pm 1.4$ )	4.8 ( $\pm 0.8$ )	14.1 ( $\pm 1.8$ )	13.2 ( $\pm 1.5$ )	14.0 ( $\pm 1.9$ )
median	39.1 (15.7...76.0)	0.8 (-1.1...2.0)	9.4 (3.9...18.1)	14.1 (-2.4...29.3)	15 (4.4...30.2)	9.1 (2.1...22.6)	4.0 (-1.1...9.3)	12.8 (0.4...26.1)	10.8 (2.6...22.0)	13.1 (-2.4...29.4)
$N$	623	623	626	643	710	608	782	689	688	688
<b>Sep–May</b>										
mean	40.8 ( $\pm 2.9$ )	0.7 ( $\pm 0.2$ )	9.4 ( $\pm 0.7$ )	25.2 ( $\pm 2.3$ )	14.9 ( $\pm 1.3$ )	5.4 ( $\pm 0.6$ )	5.8 ( $\pm 0.8$ )	8.9 ( $\pm 1.5$ )	14.6 ( $\pm 1.5$ )	17.6 ( $\pm 1.9$ )
median	26.4 (7.8...55.1)	0.7 (-1.2...2.3)	7.6 (1.4...15.9)	18.1 (-0.4...38.9)	10.0 (1.0...23.3)	4.1 (-1.8...11)	5.0 (-3.2...12.5)	8.8 (-8.8...25.2)	11.8 (-3.3...28.0)	16.2 (-4.4...35.1)
$N$	1400	1413	1426	1425	1603	1412	1310	1133	1343	1297
VOC concentration [ppb]										
<b>Jan 2013–Sep 2014</b>										
mean	3.28 ( $\pm 0.09$ )	0.10 ( $\pm 0.00$ )	0.59 ( $\pm 0.01$ )	1.05 ( $\pm 0.04$ )	1.45 ( $\pm 0.03$ )	0.10 ( $\pm 0.00$ )	0.19 ( $\pm 0.01$ )	0.14 ( $\pm 0.00$ )	0.20 ( $\pm 0.01$ )	0.22 ( $\pm 0.01$ )
median	2.58 (1.61...4.57)	0.09 (0.07...0.13)	0.51 (0.36...0.76)	0.71 (0.41...1.22)	1.30 (0.85...1.89)	0.08 (0.05...0.14)	0.13 (0.08...0.25)	0.12 (0.08...0.17)	0.14 (0.05...0.28)	0.18 (0.12...0.29)
$N$	2415	2431	2451	2477	2779	2412	2462	2139	2383	2319
<b>Jun–Aug</b>										
mean	4.27 ( $\pm 0.17$ )	0.12 ( $\pm 0.00$ )	0.60 ( $\pm 0.02$ )	1.15 ( $\pm 0.07$ )	1.88 ( $\pm 0.05$ )	0.14 ( $\pm 0.01$ )	0.11 ( $\pm 0.00$ )	0.15 ( $\pm 0.01$ )	0.12 ( $\pm 0.01$ )	0.23 ( $\pm 0.01$ )
median	3.88 (2.40...5.70)	0.12 (0.09...0.15)	0.50 (0.35...0.79)	0.79 (0.52...1.40)	1.70 (1.24...2.42)	0.12 (0.07...0.18)	0.09 (0.06...0.14)	0.13 (0.09...0.18)	0.08 (0.02...0.18)	0.19 (0.13...0.29)
$N$	748	751	756	778	863	743	938	823	826	823
<b>Sep–May</b>										
mean	2.83 ( $\pm 0.10$ )	0.09 ( $\pm 0.00$ )	0.59 ( $\pm 0.01$ )	1.00 ( $\pm 0.05$ )	1.25 ( $\pm 0.03$ )	0.09 ( $\pm 0.00$ )	0.23 ( $\pm 0.01$ )	0.13 ( $\pm 0.00$ )	0.24 ( $\pm 0.01$ )	0.22 ( $\pm 0.01$ )
median	2.14 (1.41...3.63)	0.08 (0.06...0.12)	0.51 (0.36...0.75)	0.67 (0.36...1.11)	1.09 (0.73...1.66)	0.07 (0.04...0.11)	0.17 (0.10...0.33)	0.11 (0.08...0.16)	0.17 (0.08...0.33)	0.18 (0.12...0.29)
$N$	1667	1680	1695	1699	1916	1669	1524	1316	1557	1496



**Table 4.** Statistics of measured CO and CO<sub>2</sub> fluxes and CO concentrations from each surface cover sector (3 Apr – 27 May 2014). Error estimates of the average values were calculated using the equation  $1.96 \cdot \sigma / \sqrt{N}$ , where  $\sigma$  is the standard deviation of a CO or CO<sub>2</sub> time series and  $N$  the number of data points. Lower and upper quartiles are given in parenthesis after the median values.

	All	Built	Road	Vegetation
	<hr/>			
	CO flux [ $\mu\text{g m}^{-2}\text{s}^{-1}$ ]			
mean	0.69±0.05	0.55±0.07	1.44±0.13	0.34±0.03
median	0.36 (0.11 – 0.86)	0.33 (0.06–0.75)	1.13 (0.52 – 2.06)	0.24 (0.08 – 0.46)
	CO <sub>2</sub> flux [ $\mu\text{g m}^{-2}\text{s}^{-1}$ ]			
mean	138±17	146±29	310±36	58±20
median	111 (57 – 198)	121 (68–193)	259 (129 – 424)	83 (31 – 131)
	CO concentration [ppb]			
mean	146.5±1.0	149.0±2.8	152.3±2.0	143.3±1.3
median	142.0 (133.8 – 155.9)	141.2 (133.7–155.4)	148.2 (138.7–161.3)	139.3 (131.9 – 152.5)



**Table 5.** Emission potentials ( $E_{0,\text{synth}}$ , Eq. 4) of the emission algorithm for isoprene+furan (Jun–Aug, 95% confidence intervals included). The table shows also correlation coefficients ( $r$ ), and a ratio,  $\overline{F_a}/\overline{F}$ , where  $\overline{F_a}$  is an average value given by the algorithm and  $\overline{F}$  an average value of the measurements.

	$E_{0,\text{synth}}$ [ng m <sup>-2</sup> s <sup>-1</sup> ]	$r$	$\overline{F_a}/\overline{F}$
Road	115 ± 10	0.78 ( $n = 241, p < 0.001$ )	1.01
Vegetation	140 ± 15	0.85 ( $n = 264, p < 0.001$ )	1.04
Built	125 ± 15	0.74 ( $n = 125, p < 0.001$ )	1.07

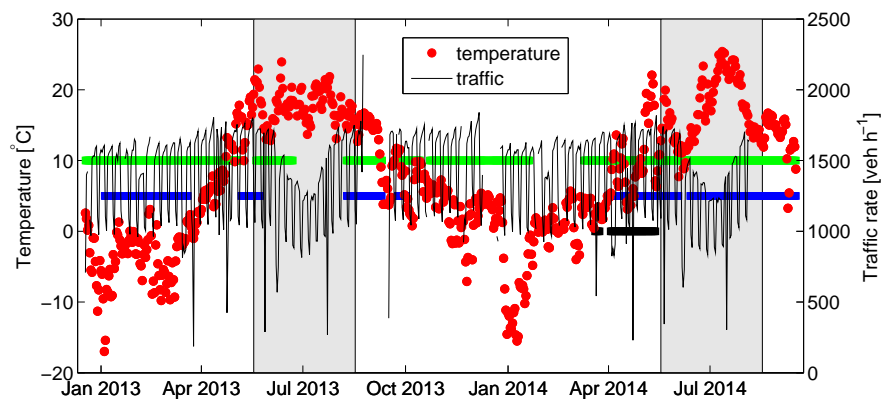


**Figure 1.** Daily averages of the ambient temperatures and traffic rates. The data coverages of PTR-MS (VOCs), Li-Cor 7000 (CO<sub>2</sub>) and LGR (CO) measurements are marked by blue, green and black lines, respectively. Grey shaded areas show periods between June–August.

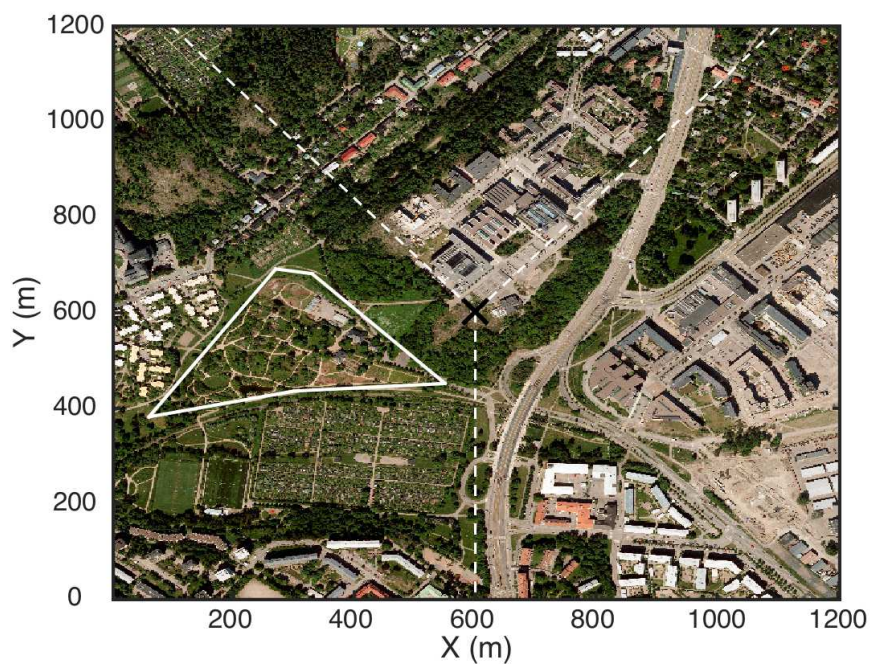


**Figure 2.** Aerial photograph of the SMEAR III station (©Kaupunkimittausosasto, Helsinki, 2011). The measurement tower is marked with a black cross. White dashed lines represent different sectors (built, vegetation, road) whereas a white solid lines border the botanical garden.

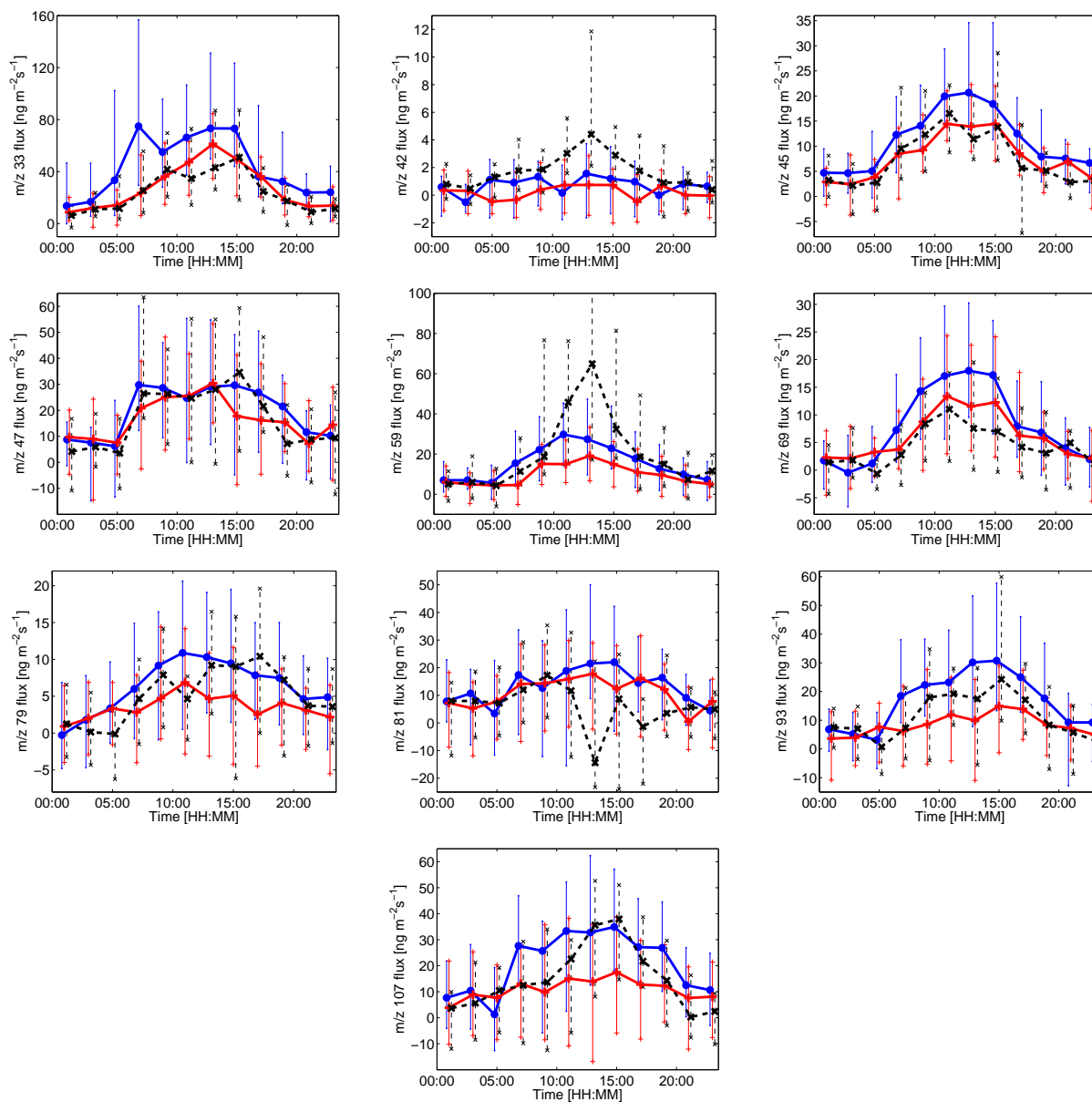


**Figure 3.** Median diurnal VOC fluxes from the three sectors for each compound excluding  $m/z$  31,  $m/z$  89 and  $m/z$  103 (Jan 2013 – Sep 2014). Blue circles, red crosses and black crosses correspond to the road sector, the vegetation sector and the built sector, respectively. Vertical lines show the lower and upper quartiles (25% and 75%). Due to sensible scaling, one upper quartile value is not shown in the  $m/z$  59 figure.

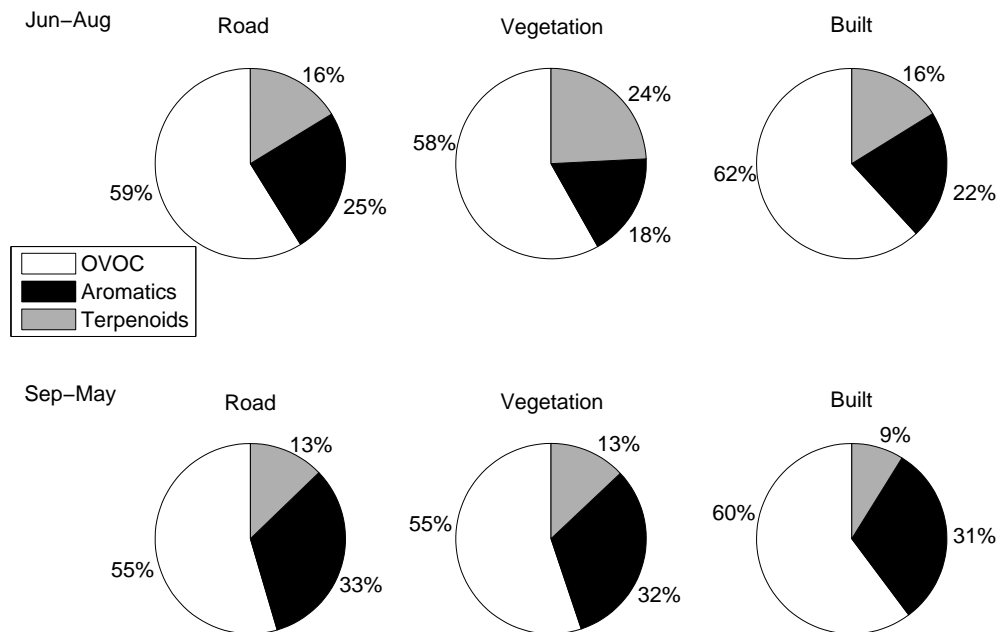


**Figure 4.** Fractions of measured OVOC (methanol, acetaldehyde, acetone+propanal), aromatic (benzene, toluene, C<sub>2</sub>-benzenes) and terpenoid (isoprene+furan, monoterpenes) fluxes from each sector in June–August and September–May (in mass basis). Ethanol+formic acid was left out from the analysis as its concentrations were not directly calibrated.

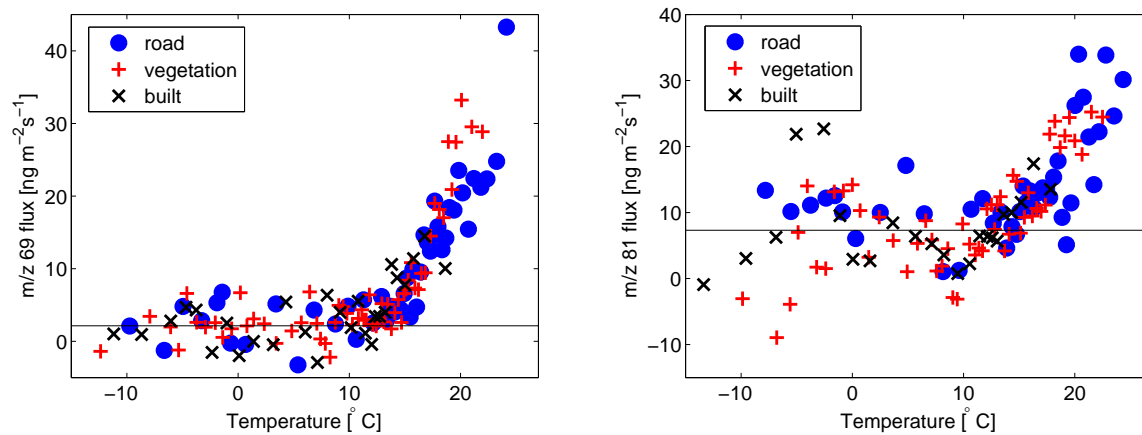


**Figure 5.** Bin-averaged isoprene+furan ( $n = 15$ ,  $m/z$  69) and monoterpene ( $n = 15$ ,  $m/z$  81) fluxes as a function of the ambient temperature from the three sectors (January 2013 – Sep 2014). Solid lines show average fluxes in the range of  $T < 10^{\circ}\text{C}$ .

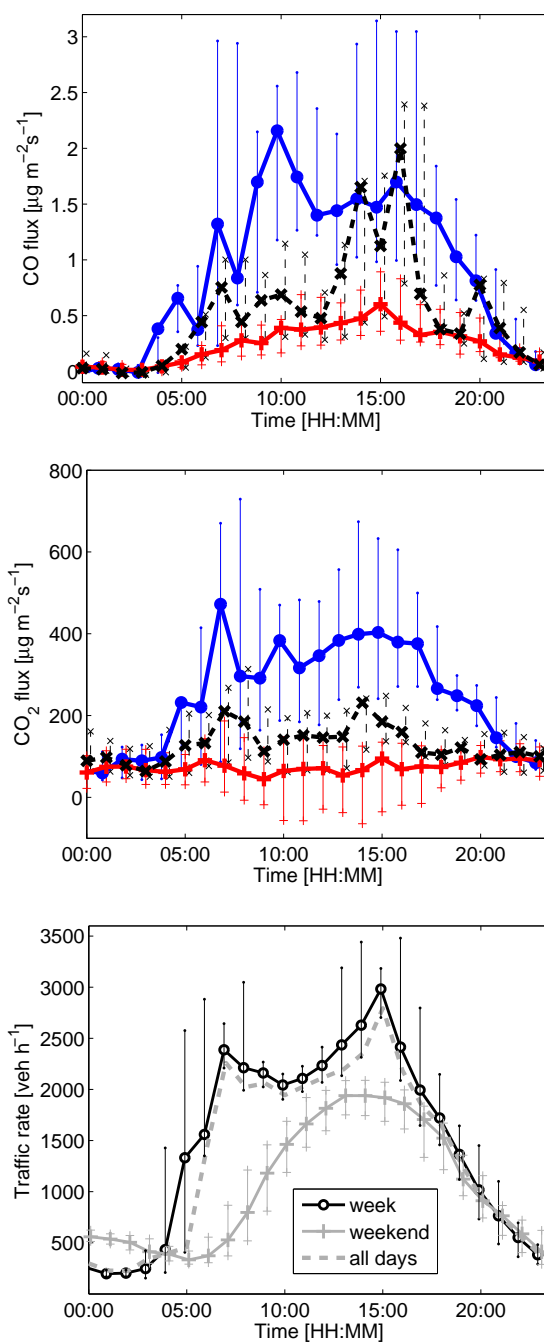


**Figure 6.** Two topmost figures present median diurnal fluxes from the three sectors for CO and CO<sub>2</sub> (3 Apr – 27 May 2014). Blue circles, red crosses and black crosses correspond to the road sector, the vegetation sector and the built sector, respectively. Vertical lines show the 25 and 75 quartiles. The lowest figure show median diurnal cycles of traffic rates from Saturday+Sunday, weekdays, and all days (Jan 2013 – Sep 2014). Vertical lines show the lower and upper quartiles for the weekend and week day values.

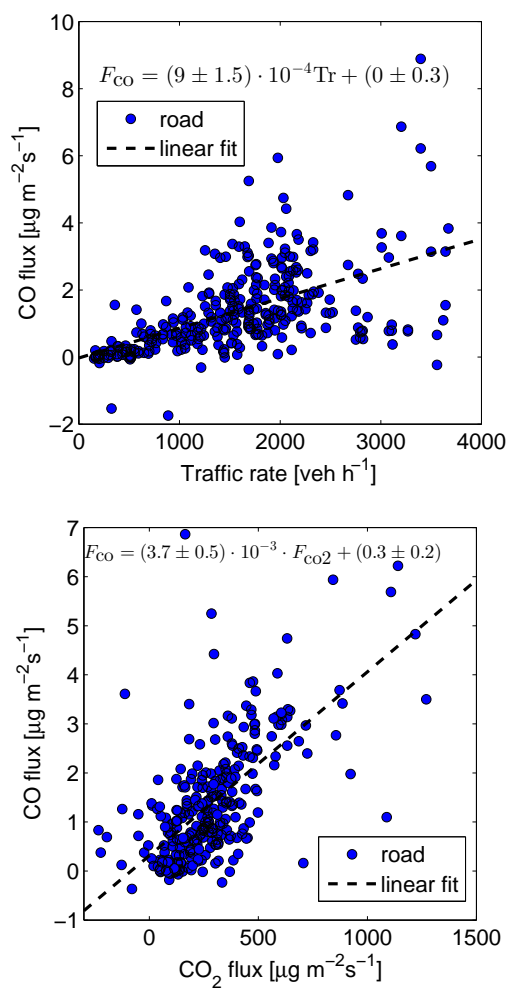


**Figure 7.** CO fluxes against traffic rates (upper figure) and CO<sub>2</sub> fluxes (lower figure) from the road sector (measured during April–May 2014).

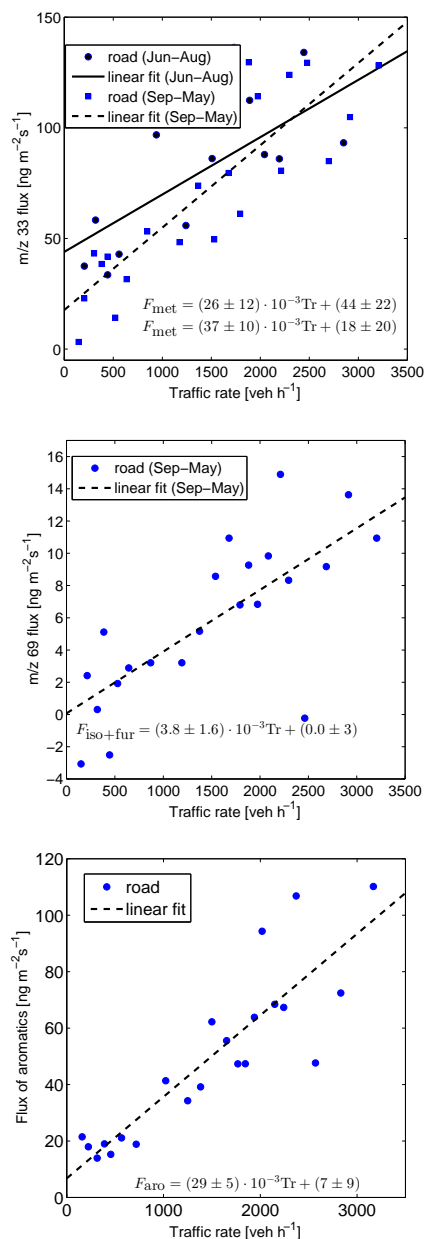


**Figure 8.** Traffic rates against methanol ( $m/z$  33, bin-averages,  $n = 15$ ), isoprene+furan ( $m/z$  69, bin-averages,  $n = 15$ ) and aromatic fluxes ( $m/z$  107, bin-averages,  $n = 30$ ) from the road section. A linear correlations between the methanol, isoprene+furan and aromatic fluxes and the traffic rates were 0.28 (Jun–Aug)/0.34 (Sep–May), 0.24 and 0.39, respectively ( $p < 0.001$ ).

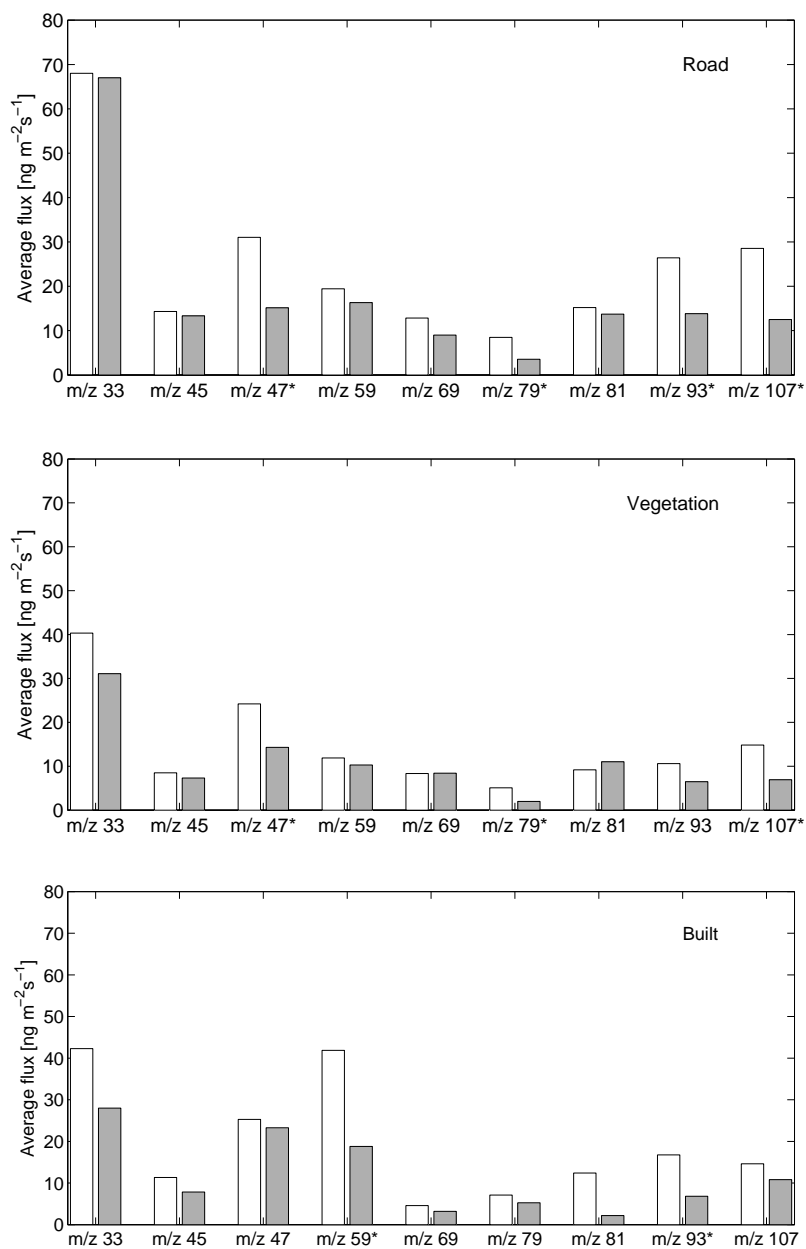


**Figure 9.** Average fluxes for each VOC (excluding acetonitrile) from Saturday+Sunday and from weekdays (Jan 2013 – Sep 2014). White and grey bars show average fluxes of weekdays and Saturday+Sunday, respectively. Asterisks in the x-axes show if differences between the average week and the average weekend fluxes were statistically significant. Uncertainties of the average fluxes were calculated using an equation  $\pm 1.96\sigma_{\text{VOC}}/\sqrt{N}$ , where  $\sigma_{\text{VOC}}$  is the standard deviation of a VOC flux time series and  $N$  the number of data points.

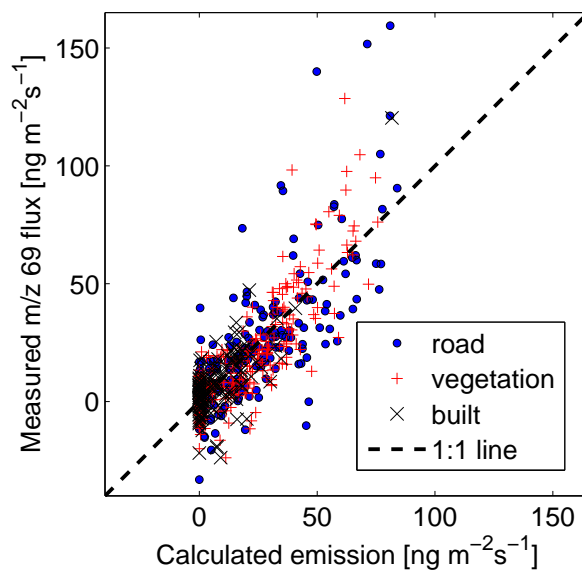


**Figure 10.** Measured isoprene fluxes vs. calculated emissions (Eqs. 4) from all sectors (Jun–Aug).

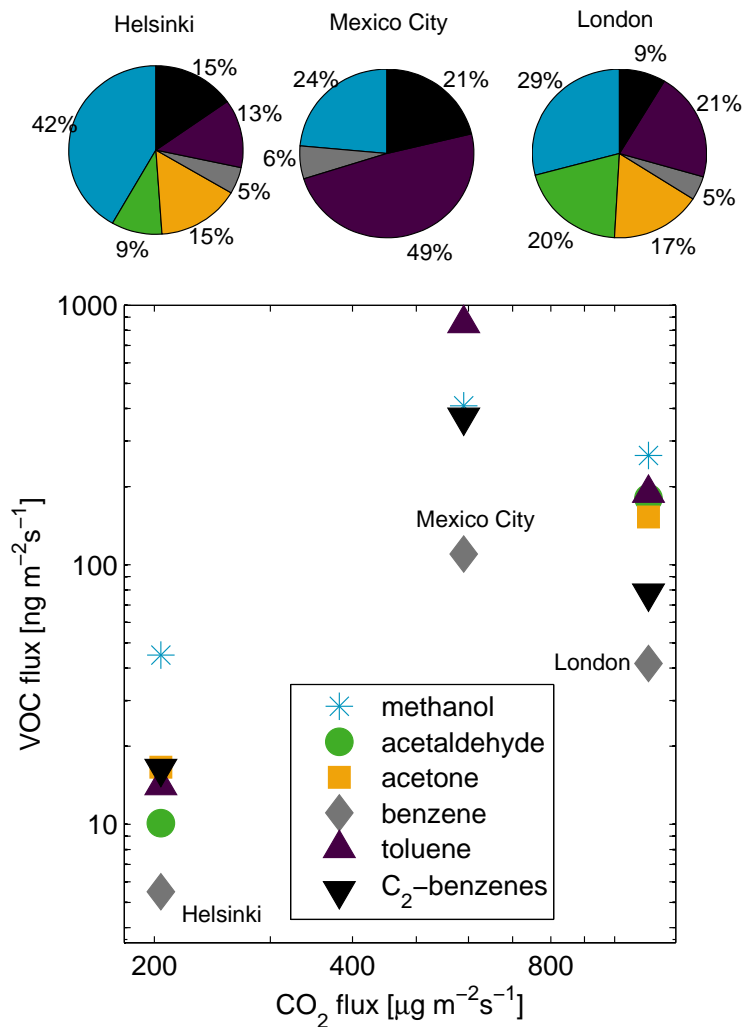


**Figure 11.** Selected VOC fluxes as a function of CO<sub>2</sub> fluxes from Helsinki, London and Mexico City (note the logarithmic scale). The average CO<sub>2</sub> and VOC fluxes of Helsinki are taken from Järvi et al. (2012) (scaled from the annual average) and this study, respectively. The corresponding average values of London are from Helfter et al. (2011) (scaled from the annual average) and Langford et al. (2010). All values of Mexico City are from MILAGRO/MCMA-2006 campaign (Velasco et al., 2009). Pie diagrams show the corresponding fractions of each compound.